haematologica
Journal of the Ferrata Storti Foundation

Multicolor detection of chronic myeloid leukemia stem cells, including novel marker CD69, predicts survival and early hematological toxicity

by Martin Culen, Marianna Romzova, Dagmar Smitalova, Tomas Loja, Daniel Busa, Ondrej Venglar, Zdenka Herudkova, Samuel Kassa, Lenka Radova, Marek Borsky, Tomas Reigl, Karla Plevova, Jiri Smejkal, Daniela Zackova, Lukas Stejskal and Jiri Mayer

Received: November 27, 2025.
Accepted: June 3, 2026.

Citation: Martin Culen, Marianna Romzova, Dagmar Smitalova, Tomas Loja, Daniel Busa, Ondrej Venglar, Zdenka Herudkova, Samuel Kassa, Lenka Radova, Marek Borsky, Tomas Reigl, Karla Plevova, Jiri Smejkal, Daniela Zackova, Lukas Stejskal and Jiri Mayer. Multicolor detection of chronic myeloid leukemia stem cells, including novel marker CD69, predicts survival and early hematological toxicity. Haematologica. 2026 June 11. doi: 10.3324/haematol.2025.300293 [Epub ahead of print]

Multicolor detection of chronic myeloid leukemia stem cells, including novel marker CD69, predicts survival and early hematological toxicity

Martin Culen[1,2], Marianna Romzova[3], Dagmar Smitalova[1], Tomas Loja[3], Daniel Busa[2], Ondrej Venglar[4,5], Zdenka Herudkova[2], Samuel Kassa[2], Lenka Radova[3], Marek Borsky[1], Tomas Reigl[3,6], Karla Plevova[1,2,3,6], Jiri Smejkal[1], Daniela Zackova[1,2], Lukas Stejskal[4], Jiri Mayer[1,2,3]

[1]Department of Internal Medicine, Hematology and Oncology, University Hospital Brno, Brno, Czech Republic

[2]Department of Internal Medicine, Hematology and Oncology, Faculty of Medicine, Masaryk University, Brno, Czech Republic

[3]Central European Institute of Technology, Masaryk University, Brno, Czech Republic

[4]Department of Hematooncology, University Hospital Ostrava, Ostrava, Czech Republic

[5]Department of Hematooncology, Faculty of Medicine, University of Ostrava, Ostrava, Czech Republic

[6]Institute of Medical Genetics and Genomics, Faculty of Medicine, Masaryk University, Brno, Czech Republic.

Running head: Multicolor detection of chronic myeloid leukemia stem cells

Correspondence: Martin Culen (mculen@gmail.com); Jiri Mayer (mayer.jiri@fnbrno.cz)

Data sharing statement: The data that supports the findings of this study is available in the supplementary material of this article. Processed microarray data is available at: https://doi.org/10.5281/zenodo.20054508. Any additional information required to re-analyze the data reported in this paper will be available from the lead contact upon request.

Conflict of interest: Zackova: advisor/consultant for Angelini, Ascentage, Enliven, Novartis, and Zentiva. Mayer: AOP Orphan Pharmaceuticals, AG Research funding, and Novartis research funding not related to this work. All remaining authors have no conflict of interest.

Acknowledgements: Figures contain icons from BioRender.com.

Funding: Supported by MH CZ - DRO (FNBr, 65269705) and MUNI/A/1733/2025. The project National Institute for Cancer Research (Programme EXCELES, ID Project No. LX22NPO5102) - Funded by the European Union - Next Generation EU. Computational resources were provided by the e-INFRA CZ project (ID:90254), supported by the Ministry of Education, Youth and Sports of the Czech Republic. We acknowledge the Flow cytometry laboratory at CEITEC MU supported by the EATRIS-CZ research infrastructure (LM2023053 funded by MEYS CR) for their support with obtaining scientific data presented in this paper.

Author contribution: Martin Culen – project design, flow and clinical data analysis, result interpretation, manuscript writing. **Marianna Romzova** – microarray gene expression experiments, project design. **Dagmar Smitalova, Zdenka Herudkova** – sample preparation, molecular analyses. **Tomas Loja, Marek Borsky** – flow cytometry. **Daniel Busa, Ondrej Venglar, Samuel Kassa** – data compilation. **Lenka Radova, Tomas Reigl, Karla Plevova** – microarray analysis and survival biostatistics. **Jiri Smejkal** – FISH analyses. **Daniela Zackova, Lukas Stejskal** – patient enrollment, clinical data consulting. **Jiri Mayer** – project design, patient enrollment, clinical data consulting, result interpretation. All authors reviewed the article.

Abstract

Chronic myeloid leukemia stem cells (LSCs) drive disease initiation, persistence, and relapse. To improve LSC-based prognostication and patient stratification, we evaluated six LSC markers (CD26, CD25, IL1-RAP, CD56, CD93, and CD69) using a single-tube analysis of CD34+CD38- cells in a cohort of 48 chronic phase chronic myeloid leukemia patients at diagnosis, month 3, or month 6. We demonstrate that these markers (including the novel marker CD69) are co-expressed, and their combination enhances LSC detection, especially during follow-up when marker expression is reduced. Furthermore, LSC data from month 3 and month 6 predict patient outcomes. We also show that quantifying residual normal hematopoietic stem cells at diagnosis enables early hematological toxicity prediction. Our findings provide technological LSC detection advancements and highlight the potential of these data for prognostic applications.

Introduction

Chronic myeloid leukemia (CML) serves as a paradigm for leukemia stem cells (LSCs).[1,2] Current understanding is that CML originates from a single aberrant stem cell, which generates further LSCs driving disease progression. Treatment-free remission (TFR) studies demonstrate that LSCs, acting as a disease reservoir, can persist even after prolonged tyrosine kinase inhibitor (TKI) therapy, posing a treatment resistance and relapse risk.[3,4]

Residual *BCR::ABL1* transcript levels only indirectly suggest LSC persistence. Direct detection relies on flow cytometry, analyzing aberrant marker expression within the stem cell-enriched CD34+CD38- compartment to distinguish LSCs from normal hematopoietic stem cells (HSCs).[5,6] The largest comparative study of 97 chronic-phase (CP) CML samples identified CD25, CD26, CD56, CD93, and IL-1RAP as the most prevalent LSC markers[7], with CD26 and IL-1RAP being the most extensively studied.[5,8–16] Studies combining markers in a single tube have demonstrated differences in LSC specificity and sensitivity between the markers.[5,15,16] However, these studies were limited to diagnosis (DX) samples, whereas follow-up LSC identification during treatment has relied solely on CD26.[9,11–14]

LSC detection in CML might offer two key advantages: i) survival prediction, and ii) improved TFR management. While CD26 has shown promise in detecting LSCs in peripheral blood (PB) during long-term follow-up (LT FU) and TFR, correlation with bulk *BCR::ABL1* levels or TFR loss remains unclear, raising questions about LSC detection accuracy in these samples.[9,13,14] Previous studies linked lower LSC counts at DX to better responses within the first 12 months of treatment.[8,15,17] However, the prognostic value of LSCs after TKI initiation remains unexplored. Additionally, early hematological toxicity has been linked to higher LSC counts and inversely linked to lower residual HSC counts at DX, suggesting that an insufficient HSC pool may be the cause rather than TKI toxicity.[17,18]

This research investigated CML LSCs using a single-tube flow cytometry approach. We analyzed LSCs in CP CML samples at DX, three months (M3), and six months (M6) after treatment, focusing on the expression of CD26, CD25, IL1-RAP, CD56, CD93, and the newly explored marker CD69. This method enabled a direct comparison of marker expression and co-expression patterns. PB samples were analyzed alongside matched bone marrow (BM) samples to evaluate LSC quantification feasibility in PB. Furthermore, we explored the clinical relevance of LSC detection by correlating LSC data with patient outcomes, including treatment response and early hematological toxicity.

Methods

Patients and samples

Patients were recruited from University Hospital Brno and University Hospital Ostrava. The study was approved by the institutional ethical committee of the University Hospital Brno (patients – no. 02-05042017/EK, donors – no. 01-27092017/EK) in accordance with the Declaration of Helsinki. All individuals signed a written informed consent prior to enrolling.

A total of 70 CML patients diagnosed in CP were enrolled (Table S1). The only selection criterion was the preferential absence of hydroxyurea pretreatment, which was administered to 9/70 (13%) patients, 1-41 days (median 3) before sampling. DX samples were collected before initiating TKI therapy.

Normal controls included BM from 7 post-allo HSCT patients (allogeneic hematological stem cell transplant; different initial diagnoses, ≤ 0.1% chimerism for ≥ 2 years) and healthy PB donors – 6 healthy individuals (not-matched with normal BM samples).

Nine cryopreserved acute myeloid leukemia (AML) samples, collected at DX, were selected based on the established CD34+CD38- cell presence.

Detailed patient and donor characteristics are provided in Table S2.

Flow cytometric LSC identification and quantification

The percentage of LSCs was calculated as % of marker positive cells from CD34+CD38- fraction. Criteria for evaluation were: a) ≥ 20 CD34+CD38- cells in DX samples and in normal control samples, b) ≥ 10 cells in M3, M6 CML samples, and c) ≥ 5 cells in LT FU CML samples. The LSC % was not evaluated in samples with less cells. The number of LSCs from mononuclear cell (MNC; $SSC^{low}CD45+$) fraction was calculated as LSC count / MNC count and $\log_{10}$ transformed. In samples with no LSCs detected, the LSC burden was calculated as 1 / MNC count to consider the presence of LSCs below our detection and sampling limits, and to allow $\log_{10}$ calculation and graphing. Only samples with ≥ 100k MNCs were evaluated.

The gating strategy is shown in Figure S1. Antibodies are specified in Table S3.

Clinical endpoints

Cumulative major molecular remission (MMR) achievement was assessed according to Hochhaus et al., where MMR achievement represented an event, censoring was performed at last contact without prior MMR, and competing events were death and TKI discontinuation without prior MMR achievement.[19] For failure free survival (FFS), failure and death of any cause were considered events. Optimum response survival (ORS) was defined as an alternative parameter, with warning, failure and death of any cause considered as events. For both FFS and ORS, censored events were the last contact or TKI discontinuation. Warning and failure events were evaluated based on *BCR::ABL1* transcript levels on International Scale, retrospectively according to European Leukemia Net 2020 guidelines.[20]

Specific hematological adverse events were assessed as follows: i) leukopenia < 4 × 10^9 leukocytes/L, ii) thrombocytopenia < 150 × 10^9 platelets/L, and iii) anemia < 120 g/L for women and < 130 g/L for men).

Statistical analyses

The survival analyzes were performed in R[21] with additional packages "survival"[22,23] and "rms"[24]. The univariate Cox model was used to assess the relationship between survival and each LSC marker. Markers with logrank p-value < 0.1 from univariate Cox analysis were considered candidates for a multivariate Cox model. The best Cox model was selected by the backward elimination of factors, using *fastbw* function. A formula for predicting survival was developed based on a linear combination of the LSC markers weighted by the regression coefficient derived from the best multivariate Cox regression model. The cut-off value was determined by using maximally selected rank statistics and represents a value corresponding to the most significant relation with outcome.

All other statistical tests were calculated in GraphPad Prism 8 software (GraphPad Software, USA).

Results

CD69 as a novel candidate CML LSC marker

To identify novel surface markers specific to CML LSCs, we performed a global RNA gene expression microarray analysis on five *de novo* CP CML samples. LSCs and HSCs were distinguished based on CD26 expression (Figure 1A). Progenitor population was included as a control and additional data source.

We identified 340 differentially expressed (DE) genes between LSCs and HSCs and 754 between progenitors and HSCs (fold change ≥ 1 and unadjusted p ≤ 0.05; Figure 1B). Stricter criteria (adjusted p ≤

0.05) yielded no DE genes between LSCs and HSCs. This indicated minimal variation within the stem cell pool and greater expression changes only as leukemic cells lose their primitive status. Following qPCR validation in 12 further CP CML cases confirmed deregulation for 7/21 (33%) selected genes in the LSC-HSC comparison and 9/10 (90%) in the progenitor-HSC comparison (Table S4). These included genes previously linked to CML pathogenesis (e.g., MYCBP2 in the mTOR pathway) or oncogenic transformation (e.g., MYB, RAD51). Importantly, we identified 18 potential DE surface marker genes in the LSC-HSC comparison (Figure 1C). We selected seven genes for flow cytometric validation in six additional *de novo* CP CML samples, based on literature reports or their involvement in potential LSC pathways (Table S5). Compared to CD26 (positive control), only CD69 showed a higher mean percentage of positive cells, although not statistically significant (Figure 1D).

Based on these results, CD69 was selected as a candidate marker for further investigation.

Comparative analysis of LSC markers at diagnosis

To identify optimal CML LSC markers, we performed multicolor flow cytometry on BM samples from 46/48 consecutive *de novo* CP CML patients from the main cohort (Figure 2A). Our panel included i) established markers: CD26, CD25, IL-1RAP, ii) candidate markers adopted from literature: CD56, CD93, and iii) our candidate marker: CD69.

Initial analysis revealed high positivity for CD69 and IL-1RAP, followed by CD25 and CD26 (Figure 2B; Figure S2). CD56 showed approximately 50% positive cells, while CD93 expression was minimal. Strikingly, CD26, CD25, IL-1RAP, and CD69 exhibited similar positivity patterns (Figure 2B) and almost perfect co-expression (Figure S3). Considering the established LSC specificity of CD26, CD25, and IL-1RAP [5,6,25], this provided indirect evidence supporting CD69 as a CML LSC marker. Notably, CD69 identified a similar number of cells as the combination of CD26, CD25, and IL-1RAP (Figure S4), suggesting its potential as a sole LSC marker at DX. However, CD69 exhibited weaker LSC-HSC discrimination than other markers (Figure 2C, D), even when testing a different antibody clone combined with a strong fluorochrome (Figure S5). Therefore, the inclusion of additional marker/s would be recommended for clear discrimination. In this regard, CD26 showed superior staining index (Figure 2D).

To assess true LSC detection, we performed indexed single-cell sorting on six cryopreserved samples, followed by *BCR::ABL1* RNA quantification (Figure 2E). CD69 showed 75% accuracy, inferior to CD26 and IL-1RAP (Figure 2F). CD25 was positive only on approximately 50% LSCs, potentially due to low marker

expression in the sample from patient CML 45. Additional CD69 fluorescence in situ hybridization (FISH) analysis (Figure S6) corroborated the molecular validation results, confirming comparable sensitivity and specificity. However, this analysis also highlighted significant inter-patient variability. Analysis of single-cell data for all markers confirmed the accuracy of our gating strategy, showing that false positivity/negativity was not caused by improper gating (Figure S7).

Finally, to determine the minimal marker combination for optimal LSC detection, we employed a stepwise approach. Combining only CD69, IL-1RAP, and either CD25 or CD26 (Figure S8) achieved efficient LSC identification. CD26 would be preferred due to its superior LSC-HSC discrimination (Figure 2D).

In conclusion, we identified CD69 as a novel CML LSC marker, suggesting a three-marker combination (CD69, IL-1RAP, and CD26) for optimal LSC detection at CP CML diagnosis.

LSC identification at early follow-up

We next assessed LSCs at M3 and M6 after initiating first-line TKI treatment. From the main cohort of 48 patients, successful phenotyping was achieved in 33 M3 and 32 M6 samples (Figure 3A).

Overall, the percentage of LSC marker-positive cells rapidly decreased, indicating the immediate therapeutic effect on the primitive CD34+CD38- population (Figure 3B, C; Figure S9). Unlike at DX, positivity was often detected by individual markers, typically IL1-RAP, rather than multiple markers. However, when additional markers were present, they were co-expressed on the same cells (Figure S10). The LSC decrease from DX to M3 and M6 was generally less pronounced than the reduction in bulk *BCR::ABL1* levels (Figure 3D) and the LSC percentages showed no significant correlation with the *BCR::ABL1* levels (Figure S11).

We also analyzed the LSC marker accuracy at the single-cell level in 5 cryopreserved samples from M3, M4, or M6, representing different response statuses (optimal, warning, and failure; Figure 3E). The individual marker specificity (absence on HSCs) remained above 75% (Figure 3F). However, sensitivity (detection of true LSCs) decreased below 50% for all individual markers, highlighting that robust LSC identification with single markers was insufficient. The low sensitivity was confirmed by projecting the *BCR::ABL1* status into dotplots, validating the LSC gating (Figure S12). Combining all six markers increased sensitivity to 75%, emphasizing the need for multi-marker panels during follow-up.

Interestingly, in two patients with samples collected at treatment failure, only 20% of CD34+CD38- cells were *BCR::ABL1*^{pos}. FISH analysis confirmed this low positivity (≤ 10%; Figure S13). However, CD34+CD38+ progenitors showed high *BCR::ABL1* positivity (64-100%), by both FISH and qPCR analysis. This suggests that LSCs may not be the primary reservoir of treatment-resistant cells early in follow-up.

Finally, we analyzed the minimum number of markers necessary for efficient LSC detection during follow-up. Marker combinations increased the percentage of detected LSCs from 10.8% with IL1-RAP alone (as the most positive marker) to 19.0% with a combination of 5/6 markers (excluding CD25) (Figure S14).

In summary, we found that LSCs are largely eradicated by M3, and their surface marker expression decreases. This complicates LSC identification during follow-up, requiring larger sample volumes and more markers in the panel.

Leukemic burden in BM versus PB

To this point, we had only analyzed the percentage of LSCs in BM. Next, we sought to compare the feasibility of LSC quantification in PB, using a combination of all six LSC markers.

Analysis of DX samples showed a higher proportion of LSCs in PB compared to paired BM samples, with a strong correlation between the two (Figure 4A). During follow-up, the average LSC percentage in PB was lower than in BM, but patient variability increased. Of the five patients with significantly higher PB LSCs than BM (Figure 4B, C), only two lost optimal response (Figure 4D), indicating no direct association with a worse prognosis. The comparison of follow-up PB and BM samples was limited to 22 paired samples, due to low CD34+CD38- cell counts post-treatment.

Previous studies have indicated that the fraction of LSCs in all leukocytes is prognostically relevant in AML.[26] Thus, we aimed to analyze this as an alternative LSC quantification parameter. We normalized LSCs to MNC fraction (LSC n/MNC, also termed leukemic burden) since our M3 and M6 samples were primarily analyzed after cryopreservation and lacked granulocytes (Figure S15). To provide a broader context, we also analyzed LT FU samples from CP CML patients, AML DX samples, and material from healthy donors to analyze false positivity (LSC marker expression on HSCs). For simplicity, we refer to normal stem cells expressing LSC markers as LSCs in this context. The leukemic burden could be quantified in more samples than the LSC %, where the LSC acquisition thresholds were often not met in CML follow-up samples with low LSC counts. Overall, the two metrics showed a good correlation (with the best match at DX),

suggesting their possible interchangeability (Figure S16). The LSC burden correlated with bulk *BCR::ABL1* transcript levels at DX, both for PB and BM, but not in M3, M6 or LT FU samples (Figure S17). The numbers of acquired MNCs are shown in Figure S18.

DX CML samples presented a high LSC burden in the BM, comparable to AML samples (Figure 4E). This was also evident in PB, suggesting an efflux into PB, especially given the significantly lower CD34+ frequency in PB (Figure 4E; Figure S19). At M3 and M6 the LSC burden decreased to levels similar to normal controls, both in BM and PB. Interestingly, no further decline was observed in LT FU (analyzed only in PB). The LT FU samples consisted of two cohorts: a) 10/48 main cohort patients collected at 2-5 years (median 3 years) from TKI initiation; and b) 11 additional CP CML patients collected at 3-19 years (median 7 years) from TKI initiation. Notably, both cohorts demonstrated a similar LSC burden, despite the fact that 7/10 patients from the first cohort were in MMR at sampling, while all patients in the second cohort were selected to have been in MMR or better for at least 2 years (range 2-10, median 5 years).

In summary, our findings indicate that LSC quantification in PB is feasible at diagnosis but becomes challenging at M3 and M6 due to low post-treatment LSC levels in PB. This situation may require the analysis of larger sample volumes to detect sufficient LSCs in PB. Using the LSC n/MNC parameter, we demonstrated that the LSC burden persists at similar levels from M3 to several years of treatment, irrespective of the molecular response depth.

LSC data from M3 and M6 predict prognosis

To assess the potential prognostic value, we correlated LSC data with three clinical endpoints in 48 patients from the main cohort. These endpoints included MMR and FFS, and ORS achievement established here as a more sensitive alternative to FFS (Figure 5A). Patients were followed from February 2017 to March 2024, with a follow-up period of 22-77 months (median 61 months) for 41 surviving patients; 7 patients died (2 CML-related, 4 non-CML related, 1 unknown). LSCs were quantified using the 6 individual LSC markers or their union, expressed as both LSC % and LSC n/MNC. PB *BCR::ABL1* transcript levels served as a reference parameter, though acknowledging a positive bias since MMR, FFS, and ORS are directly based on this parameter.

Initially, we correlated LSC data from BM samples. DX LSC data showed minimal correlation with the three clinical outcomes (Figure 5B; Figure S20). The strongest association with prognosis was observed with LSC data from M3, and to a lesser extent from M6. Similarly, *BCR::ABL1* transcript levels were linked to

prognosis at M3 and M6 but not at DX. MMR achievement was mainly linked to M3 LSC n/MNC, while FFS and ORS correlated with various LSC % and LSC n/MNC parameters from both M3 and M6. CD26, CD25, and CD69 were the most predictive individual markers; IL1-RAP and CD56 showed no prognostic value. No overall difference was observed between LSC % and LSC n/MNC data. Multivariate analysis developed three models where the addition of LSC data improved patient prognostication over *BCR::ABL1* alone – FFS prediction based on M3 data and ORS prediction based on M3 and M6 data (Figure 5C; Figure S21A). The ORS prediction models were successfully validated by both Akaike information criteria and Brier score, demonstrating improved predictive performance compared to *BCR::ABL1* without LSC data (Figure S21B, C). No model could be developed using only LSC data, suggesting LSC quantification as a supplementary parameter to standard *BCR::ABL1* quantification.

Prognosis correlating with PB LSC data was primarily limited to LSC n/MNC parameters due to limited LSCs, particularly at M3 and M6. Even with LSC n/MNC, the prognostic relationship was weaker than BM (Figure S22).

In summary, LSC frequencies at M3 and M6 are linked to patient prognosis, providing additional prognostic information beyond standard *BCR::ABL1* assessment.

Residual HSCs predict hematological toxicity

Following TKI treatment, the surviving HSCs are expected to replace the *BCR::ABL1*^{pos} clone and restore normal hematopoiesis. We investigated whether patients with fewer surviving HSCs (CD34+CD38- cells negative for all LSC markers) experience impaired hematopoietic reconstitution.

As a first step, we analyzed the incidence of TKI treatment reductions or interruptions (TKI R/Is) due to hematological adverse events (hAEs) in the main cohort (n = 48). This represented clinically relevant hematological toxicity based on clinicians' decisions. TKI R/Is occurred early in treatment (9/10 events within the first three months; Figure 6A), limiting our predictive analysis to HSC data from DX. BM DX HSCs were quantified as: i) the percentage of HSCs in the CD34+CD38- fraction (HSC %), ii) the number of HSCs per MNC fraction (HSC n/MNC), and iii) the number of HSCs per milliliter of BM (HSC n/ml). The HSC n/MNC and HSC n/ml parameters showed a link to TKI R/I incidence (Figure 6B). Interestingly, no relationships were found for individual hAEs (leukopenia, thrombocytopenia, and anemia), except for lower HSC n/ml in patients experiencing thrombocytopenia (Figure S23). Refining the analysis to more

primitive CD34+CD38-CD90+ cells or HSC quantification in PB provided no link with TKI R/I (Figure S24 and S25).

These findings confirm that a higher HSC load is associated with a lower risk of hematological toxicity, likely due to an improved capacity for hematopoietic reconstitution.

Discussion

This study uniquely compares six CML LSC markers across diagnosis, early (M3, M6), and late (years 2-19) follow-up samples. Our single-tube analysis, confirmed by single-cell molecular analysis, reveals novel co-expression patterns and highlights CD69 as a top-performing marker. Combining multiple markers is crucial for reliable LSC detection, especially in follow-up samples with low individual marker expression. LSC data, particularly at M3/M6 with markers CD26, CD25, and CD69, demonstrates prognostic potential. Furthermore, HSC quantification at CML DX predicts early hematological toxicities.

CD69, a known lymphocyte activation marker, exhibits expression dependent on *BCR::ABL1* function.[27,28] While previous larger screens included CD69, its significance was not recognized.[7,29] Although CD69 did not exhibit the highest separation index between LSCs and HSCs in our study, it ranked among the top markers for LSC identification and prognostic relevance. CD26 consistently demonstrated high LSC sensitivity and prognostic relevance, in line with its current status as the most widely used CML LSC marker. IL1-RAP showed a high positivity in M3 and M6 with similar accuracy to CD69, but intriguingly without a clear prognostic association. CD25 identified only a subset of cells, consistent with previous findings by Landberg et al.[15,16] Unlike Herrmann et al., who reported high CD56 positivity on CML LSCs at DX [7], our findings showed that CD56 identified approximately half as many LSCs as CD26. However, in FU, CD56 expression was observed on samples without expression of other markers (Figure 3B). CD93 was initially proposed as a marker for LSCs within the CD34+CD38-CD90+ fraction.[30] Herrmann et al. later reported approximately 75% CD93+ cells also in CD34+CD38- fraction.[7] We hypothesize that the poor performance of CD93 in our study may be attributed to an inappropriate antibody clone. Unfortunately, at our data's collection, the results from Herrmann et al. were not published. Therefore, we did not test alternative CD93 antibodies to reach similar efficacy. In general, exploration of different antibody manufacturers and clones when establishing new LSC panels is recommended and represents a limitation of the current study.

The correlation of LSC data with clinical endpoints revealed that LSC quantification at M3 or M6 stages is superior to that at DX. This is consistent with the established clinical use of *BCR::ABL1* transcript levels in

risk stratification.[31] We observed that only certain LSC markers demonstrated prognostic relevance, which may be related to their identification accuracy. The BM LSC data provided superior prognostic relevance to PB, which might be due to higher LSC frequencies in BM post-treatment. Further prognostic validation on larger patient cohorts is now required to select the LSC markers with the greatest prognostic value and to determine the exact benefit beyond routine bulk *BCR::ABL1* quantification.

The growing trend of TKI cessation underscores the need to accurately predict TFR using LSC detection. Previous studies using CD26 found no correlation between persistent LSC quantity and *BCR::ABL1* levels or TFR loss [13,14], but our findings suggest that incorporating additional markers could improve detection accuracy. Furthermore, LSC quantification in TFR has predominantly relied on PB samples due to the decreased use of BM aspiration. However, our study highlights the inherent difficulty in detecting LSCs in PB post-TKI therapy, as the PB LSC burden is approximately one log lower than in BM. This is consistent with Ilhan et al.'s findings of undetectable LSCs in 4 ml of PB versus 2 ml of BM at deep molecular response.[11] Our results indicate that LSC burden does not decrease further beyond M6, corroborating findings of others who extended analyses even to TFR samples.[12,13,32] This suggests the applicability of our conclusions for TFR, highlighting the need for multi-marker LSC detection and the BM sample superiority in LSC detection and prognostication. To our knowledge, our data represents the first direct comparison of multiple markers in a follow-up setting. Future research should focus on similar multi-parametric LSC analysis in TFR, ideally with concurrent PB and BM sampling, to comprehensively evaluate the relationship between persistent LSCs and TFR outcomes.

Previous studies indicated decreased hAE risk in patients harboring more residual HSCs, as quantified by FISH.[17,18] Our flow cytometric analysis at DX confirms this relationship. These findings support the hypothesis that hematological toxicity stems not from TKIs themselves, but from insufficient hematological reconstitution in patients with limited surviving HSCs after TKI clone clearance. This is supported by the high hAE frequency in first-line imatinib and nilotinib treatment, contrasting with their near absence upon treatment re-initiation after TFR loss.[3,4,33] Similarly, imatinib treatment for gastrointestinal tumors showed adverse hematological events in less than 10% of patients.[34] Taken together, early hematological toxicity should not necessitate TKI reduction or interruption and dose modifications could be performed only after response achievement, similar to with venetoclax/azacitidine in AML.[35]

Based on our data and acknowledging the need for further validation on larger prospective cohorts, we propose the following for the practical application of LSC/HSC measurements. LSC panel: Utilize a panel

of 2-6 antibodies. Key markers include CD26 (for high LSC/HSC separation capacity and prognostic value) and CD69 (for high LSC detection capacity and prognostic value). Additional markers can be optionally included to enhance LSC detection, mainly in follow-up. Potential uses: At DX, HSC quantification can predict early hAEs. At M3 and M6, LSC detection can improve prognostication. At LT FU, LSC detection could possibly improve patient selection for TKI discontinuation and subsequent TFR monitoring. Sample requirements: Acquiring approximately 100 CD34+CD38- cells should ensure robust LSC/HSC identification, but this target may not be consistently met due to the variable distribution of this fraction (Figure 4E). For simplicity, we advocate for analyzing fixed sample volumes. Based on our fresh sample data, (Figure S26), we propose the following collections: For DX BM, a median of 5000 CD34+CD38- cells/mL BM was observed, making analysis of 100 µL BM sufficient. BM is the material of choice at DX as it is standardly collected, and PB HSCs did not correlate with hAE occurrence. For follow-up samples, a median of 162 CD34+CD38- cells/mL was found in BM at M3 and M6 and 16 CD34+CD38- cells/mL in PB at LT FU. Thus, we recommend analyzing 1-5 mL of BM or 5-10 mL of PB. BM is preferred as the primary reservoir for LSCs during treatment; however, its collection is not currently standard of care and thus not routinely available. It is important to note that reported frequencies of the CD34+CD38- population can vary across reports due to differing CD38- gating stringency. Therefore, our recommendations are based on our own measurements, despite the limited number of freshly processed M3+M6 samples.

References

1. Faderl S, Talpaz M, Estrov Z, O'Brien S, Kurzrock R, Kantarjian HM. The biology of chronic myeloid leukemia. N Engl J Med. 1999;341(3):164-172.

2. Melo JV, Barnes DJ. Chronic myeloid leukaemia as a model of disease evolution in human cancer. Nat Rev Cancer. 2007;7(6):441-453.

3. Mayer J. Treatment cessation in chronic myeloid leukemia: evidence and uncertainties. Hematol Oncol. 2025;43(6):e70155.

4. Mahon F-X, Pfirrmann M, Dulucq S, et al. European Stop Tyrosine Kinase Inhibitor Trial (EURO-SKI) in Chronic Myeloid Leukemia: Final Analysis and Novel Prognostic Factors for Treatment-Free Remission. J Clin Oncol. 2024;42(16):1875-1880.

5. Jaras M, Johnels P, Hansen N, et al. Isolation and killing of candidate chronic myeloid leukemia stem cells by antibody targeting of IL-1 receptor accessory protein. Proc Natl Acad Sci U S A. 2010;107(37):16280-16285.

6. Herrmann H, Sadovnik I, Cerny-Reiterer S, et al. Dipeptidylpeptidase IV (CD26) defines leukemic stem cells (LSC) in chronic myeloid leukemia. Blood. 2014;123(25):3951-3962.

7. Herrmann H, Sadovnik I, Eisenwort G, et al. Delineation of target expression profiles in CD34+/CD38− and CD34+/CD38+ stem and progenitor cells in AML and CML. Blood Adv. 2020;4(20):5118-5132.

8. Culen M, Borsky M, Nemethova V, et al. Quantitative assessment of the CD26+ leukemic stem cell compartment in chronic myeloid leukemia: patient-subgroups, prognostic impact, and technical aspects. Oncotarget. 2016;7(22):33016-33024.

9. Bocchia M, Sicuranza A, Abruzzese E, et al. Residual peripheral blood CD26+ leukemic stem cells in chronic myeloid leukemia patients during TKI therapy and during treatment-free remission. Front Oncol. 2018;8:194.

10. Raspadori D, Pacelli P, Sicuranza A, et al. Flow cytometry assessment of CD26+ leukemic stem cells in peripheral blood: a simple and rapid new diagnostic tool for chronic myeloid leukemia. Cytometry B Clin Cytom. 2019;96(4):294-299.

11. Ilhan O, Narli Ozdemir Z, Dalva K, et al. Leukemic stem cells shall be searched in the bone marrow before "tyrosine kinase inhibitor-discontinuation" in chronic myeloid leukemia. Int J Lab Hematol. 2021;43(5):1110-1116.

12. Ebian HF, Abdelnabi A-SM, Abdelazem AS, Khamis T, Fawzy HM, Hussein S. Peripheral blood CD26 positive leukemic stem cells as a possible diagnostic and prognostic marker in chronic myeloid leukemia. Leuk Res Rep. 2022;17:100321.

13. Pacelli P, Santoni A, Sicuranza A, et al. Prospective monitoring of chronic myeloid leukemia patients from the time of TKI discontinuation: the fate of peripheral blood CD26+ leukemia stem cells. Front Pharmacol. 2023;14:1194712.

14. Camacho MF, Peña M, Toloza MJ, et al. Evaluation of leukemic stem cell (CD26 +) in chronic myeloid leukemia patients with different molecular responses and in treatment-free remission. Clin Exp Med. 2025;25(1):93.

15. Landberg N, Hansen N, Askmyr M, et al. IL1RAP expression as a measure of leukemic stem cell burden at diagnosis of chronic myeloid leukemia predicts therapy outcome. Leukemia. 2016;30(1):253-257.

16. Landberg N, von Palffy S, Askmyr M, et al. CD36 defines primitive chronic myeloid leukemia cells less responsive to imatinib but vulnerable to antibody-based therapeutic targeting. Haematologica. 2018;103(3):447-455.

17. Mustjoki S, Richter J, Barbany G, et al. Impact of malignant stem cell burden on therapy outcome in newly diagnosed chronic myeloid leukemia patients. Leukemia. 2013;27(7):1520-1526.

18. Janssen JJWM, Deenik W, Smolders KGM, et al. Residual normal stem cells can be detected in newly diagnosed chronic myeloid leukemia patients by a new flow cytometric approach and predict for optimal response to imatinib. Leukemia. 2012;26(5):977-984.

19. Hochhaus A, Wang J, Kim D-W, et al. Asciminib in newly diagnosed chronic myeloid leukemia. N Engl J Med. 2024;391(10):885-898.

20. Hochhaus A, Baccarani M, Silver RT, et al. European LeukemiaNet 2020 recommendations for treating chronic myeloid leukemia. Leukemia. 2020;34(4):966-984.

21. R Core Team. The R Project for Statistical Computing. Available at https://www.R-project.org/ Accessed May 6, 2026.

22. Therneau TM. A Package for Survival Analysis in R. Available at https://CRAN.R-project.org/package=survival Accessed May 6, 2026.

23. In: Therneau TM, Grambsch PM. Modeling survival data: extending the Cox model. New York: Springer; 2000.

24. Harrell Jr FE. rms: Regression Modeling Strategies. Available at https://CRAN.R-project.org/package=rms Accessed May 6, 2026.

25. Sadovnik I, Hoelbl-Kovacic A, Herrmann H, et al. Identification of CD25 as STAT5-dependent growth-regulator of leukemic stem cells in ph+ CML. Clin Cancer Res. 2016;22(8):2051-2061.

26. Zeijlemaker W, Grob T, Meijer R, et al. CD34+CD38- leukemic stem cell frequency to predict outcome in acute myeloid leukemia. Leukemia. 2019;33(5):1102-1112.

27. Sancho D, Gómez M, Sánchez-Madrid F. CD69 is an immunoregulatory molecule induced following activation. Trends Immunol. 2005;26(3):136-140.

28. Hantschel O, Gstoettenbauer A, Colinge J, et al. The chemokine interleukin-8 and the surface activation protein CD69 are markers for Bcr-Abl activity in chronic myeloid leukemia. Mol Oncol. 2008;2(3):272-281.

29. Warfvinge R, Geironson L, Sommarin MNE, et al. Single-cell molecular analysis defines therapy response and immunophenotype of stem cell subpopulations in CML. Blood. 2017;129(17):2384-2394.

30. Kinstrie R, Horne GA, Morrison H, et al. CD93 is expressed on chronic myeloid leukemia stem cells and identifies a quiescent population which persists after tyrosine kinase inhibitor therapy. Leukemia. 2020;34(6):1613-1625.

31. Cross NCP, Ernst T, Branford S, et al. European LeukemiaNet laboratory recommendations for the diagnosis and management of chronic myeloid leukemia. Leukemia. 2023;37(11):2150-2167.

32. Bocchia M, Sicuranza A, Pacelli P, et al. Peripheral blood CD26+ leukemia stem cells monitoring in chronic myeloid leukemia patients from diagnosis to response to TKIs: Interim results of a multicenter prospective study (PROSPECTIVE FLOWERS). Blood. 2020;136(Supplement 1):45-46.

33. Saglio G, Kim D-W, Issaragrisil S, et al. Nilotinib versus imatinib for newly diagnosed chronic myeloid leukemia. N Engl J Med. 2010;362(24):2251-2259.

34. Demetri GD, Mehren M von, Blanke CD, et al. Efficacy and safety of imatinib mesylate in advanced gastrointestinal stromal tumors. N Engl J Med. 2002;347(7):472-480.

35. European Medicines Agency. Venclyxto : EPAR - Product Information. Available at https://www.ema.europa.eu/en/documents/product-information/venclyxto-epar-product-information_en.pdf Accessed May 6, 2026.

Table 1. Suggested application of LSC/HSC measurements in practice.

	DX	**M3 and M6**	**TFR**
LSC panel, n markers	2-3	2-5	2-5
Material (lyse-wash-stain)	0.1 ml BM	1-5 ml BM or 5-10 ml PB	1-5 ml BM or 5-10 ml PB
Application	early hAE prediction	prognostication	patient selection, MRD monitoring

BM – bone marrow, DX – diagnosis, hAE – hematological adverse event, LSC – leukemic stem cell, M – month, MRD – minimal residual disease, PB – peripheral blood, TFR – treatment free remission.

Figure 1. Identification of novel CML LSC surface markers. A – Workflow. BM samples were FACS sorted based on CD26 expression into LSCs (CD34+CD38-CD26+) and HSCs (CD34+CD38-CD26-), plus a progenitor fraction (CD34+CD38+). Gene expression was compared in LSCs vs. HSCs and in progenitors vs. HSCs. qPCR and FACS validation were performed on additional BM diagnosis samples for selected genes. B – Overall gene-expression shown for LSCs vs. HSCs and progenitors vs. HSCs, with non-adjusted p values. C – The most deregulated surface marker genes on LSCs. The genes with a color font were chosen for FACS validation. D – FACS validation of selected surface markers, with CD26 used as a positive control. Mean, one-way, non-parametric ANOVA. BM – bone marrow. CP CML – chronic phase myeloid leukemia. FACS – fluorescence activated cell sorting. HSC – normal stem cells. LSC – leukemic stem cells. qPCR – quantitative PCR. ** $p < 0.01$.

Figure 2. Comparison of LSC markers in BM at CML diagnosis. A – Scheme and sample counts. B – Heatmap showing the % of positive cells according to different markers in the CD34+CD38- fraction, along with basic clinical data below. C – Separation capacity for LSCs and HSCs of individual markers, demonstrated on patient CML 16. D – Separation index of individual markers. Inclusion criterion of ≥ 5 cells in both marker+ and marker- fraction passed by n samples indicated in the graph. Mean ± SD. CD26 compared with other markers using unpaired, non-parametric one-way ANOVA, only statistically significant results shown. The equation shows separation index calculation. E, F – Single cell analysis of *BCR::ABL1* RNA expression in 6/39 main cohort patients. F – Specificity, sensitivity, and accuracy of LSC surface markers, shown as average of all analyzed cells from E. BM – bone marrow, CP CML – chronic phase myeloid leukemia, DX – diagnosis, ELTS – EUTOS long-term survival score, LSC – leukemic stem cell, M – month, MMR – major molecular response, n – number/count, ns – not significant, TKI – tyrosine kinase inhibitor. *** $p < 0.001$, **** $p < 0.0001$.

Figure 3. Comparison of LSC markers in BM at M3 and M6 after starting TKI treatment. A – Scheme and sample numbers. B – Heatmap showing the % of positive cells according to different markers in the CD34+CD38- fraction and the % of cells with non-coexpressed markers shown as Δ (difference between the union gate and the best ranking marker). Basic clinical parameters shown below. C – Decline of LSC % in CD34+CD38- fraction. D – Decline of *BCR::ABL1* % determined by molecular analysis in bulk peripheral blood. C, D – Only patients with at least two time points shown, n = 37. DX-M3 line color determined by M3 response, M3-M6 line color by M6 response. Unpaired, non-parametric one-way ANOVA, only statistically significant results shown. E, F – Analysis of *BCR::ABL1* RNA expression in single cells sorted

from cryopreserved samples of 5/39 main cohort patients. G – Specificity, sensitivity, and accuracy of LSC surface markers, shown as average of all analyzed cells from E. BM – bone marrow, CP CML – chronic phase myeloid leukemia, DX – diagnosis, IS – international scale, LSC – leukemic stem cell, M – month, MMR – major molecular response, n – number/count, TKI – tyrosine kinase inhibitor. ** $p < 0.01$, **** $p < 0.0001$.

Figure 4. Quantification of LSCs in PB and in the MNC fraction. A, B – Comparison of LSC % in CD34+CD38- fraction in matched BM and PB samples of 31 CP CML patients from the main cohort, shown A – at diagnosis, B – at M3 plus M6 together. BM compared with PB using non-parametric paired t-test: ** denotes statistical significance at DX. Correlation: linear regression and Spearman correlation. C – Example of discrepancy between BM and PB LSC %, shown for CML 52, M6 (red dot in panel B). D – Survival data for the most discrepant samples from B (encircled), showing achievement of MMR and survival summary. E – Quantification of LSCs as a fraction of MNCs. Gray, background circles show the fraction of all CD34+CD38- cells from MNCs. DX, M3, M6: matched BM-PB pairs, patients from the main CML cohort. LT FU: PB samples from long-term follow-up. LT FU a: main cohort patients, year 2-5 from diagnosis, 7/10 in MMR at sampling. LT FU b: additional CP CML patients, year 2-10 from diagnosis, all in MMR or better at sampling. NC: PB and BM from non-matched donors. AML: BM samples from diagnosis. Median, non-parametric, paired or unpaired t-test. AML – acute myeloid leukemia, BM – bone marrow, CP CML – chronic phase chronic myeloid leukemia, DX – diagnosis, LSC – leukemic stem cell, M – month, MMR – major molecular response, MNC – mononuclear cells, NC – normal control, ns – not significant, PB – peripheral blood. * $p < 0.05$, ** $p < 0.01$, *** $p < 0.001$, **** $p < 0.0001$.

Figure 5. Prognostic value of BM LSC data. A – Three clinical endpoints evaluated in the main CP CML cohort; Kaplan-Meier curves. B – Univariate analysis results showing the parameters with statistically significant link to prognosis. LSC parameters and *BCR::ABL1* transcript levels from three timepoints correlated with the three clinical endpoints. C – Multivariate analysis showing the best multivariate Cox regression models. B, C – LSC data evaluated both as % of LSCs from CD34+CD38- fraction (LSC %) or number of LSCs from MNC fraction (LSC n). LSC identification performed based on individual markers or the 6 marker union (positivity for any marker). International scale *BCR::ABL1* transcript levels from PB used. BM – bone marrow, CI – confidence interval, DX – diagnosis, FFS – failure-free survival, HR – hazard ratio, LSC – leukemic stem cell, M – month, MMR – cumulative major molecular response, MNC – mononuclear cells, n – number, NA – not available, ORS – optimum response survival.

Figure 6. Correlation of residual BM HSCs with hematological toxicity in the main 48 CP CML patient cohort. A – cumulative TKI R/I incidence based on hematological toxicity. B – comparison of BM HSC levels at diagnosis between patients with and without TKI R/I within the first three 3 months. HSCs were identified as CD34+CD38- cells lacking expression of any of the 6 LSC markers. HSCs quantified as: percentage of CD34+CD38- fraction (HSC %, left), fraction of MNCs (HSC n/MNC, middle), and HSC count per 1 ml of BM (HSC n/ml, right). Median, unpaired, non-parametric t-test. BM – bone marrow, CP CML – chronic phase chronic myeloid leukemia, HSC – normal hematopoietic stem cell, LSC – leukemic stem cell, MNC – mononuclear cell, n – number/count, ns – not significant, TKI R/I – tyrosine kinase inhibitor dose reduction or treatment interruption. ** $p < 0.01$.

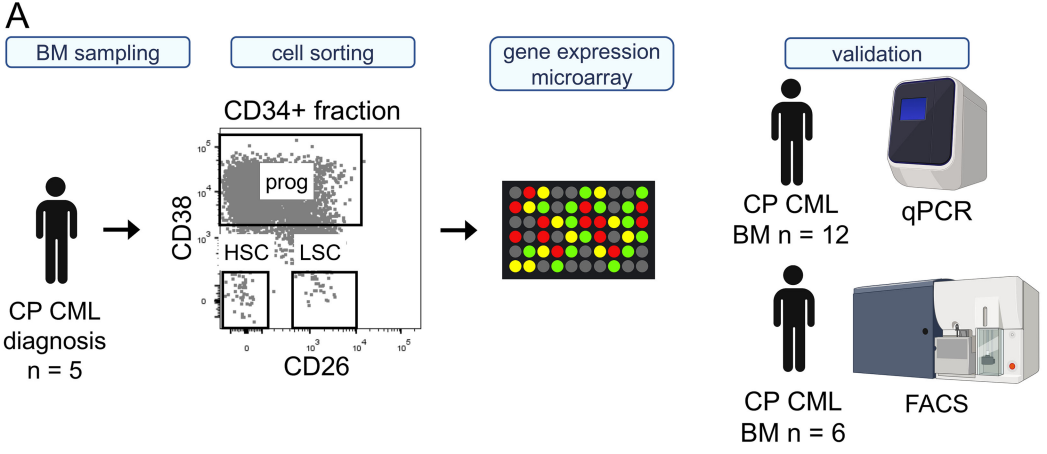

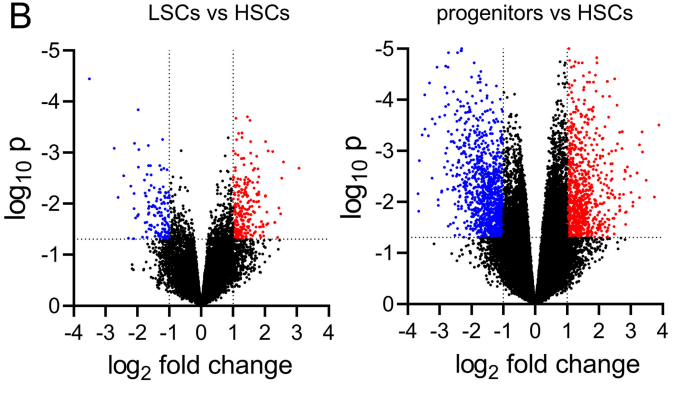

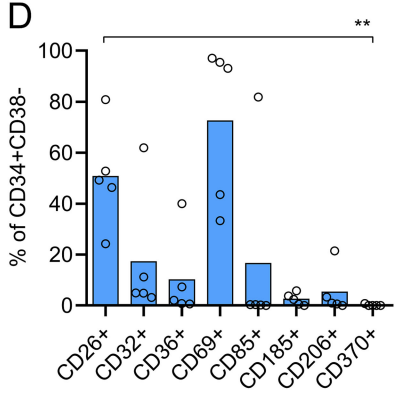

C

CD molecule	antigen	log2 fold change	p	full name
CD36	GPIV	1.89	0.022	CD36 molecule
CD370	CLEC9A	1.85	0.042	C-type lectin domain containing 9A
CD25	IL2RA	1.77	0.004	interleukin 2 receptor subunit alpha
CD32	FCGR2A	1.62	0.026	Fc fragment of IgG receptor Iia
CD233	SLC4A1	1.46	0.010	solute carrier family 4 member 1
CD206	MRC1	1.39	0.044	mannose receptor C-type 1
CD85D	LILRB2	1.35	0.006	leukocyte immunoglobulin-like receptor B2
CD26	DPP4	1.28	0.017	dipeptidyl peptidase 4
CD225	IFITM1	1.25	0.012	interferon induced transmembrane protein 1
CD36L2	SCARB2	1.13	0.004	scavenger receptor class B member 2
CD69	CLEC2C	0.98	0.025	CD69 molecule
CD62L	SELL	-1.00	0.008	selectin L
CD110	MPL	-1.15	0.033	MPL proto-oncogene, thrombopoietin receptor
CD209	DC-SIGN1	-1.23	0.036	CD209 molecule
CD164	MUC-24	-1.30	0.012	CD164 molecule
CD117	KIT	-1.33	0.015	KIT proto-oncogene, receptor tyrosine kinase
CD185	CXCR5	-1.63	0.011	C-X-C motif chemokine receptor 5
CD42C	GP1BB	-2.21	0.005	glycoprotein Ib platelet subunit beta

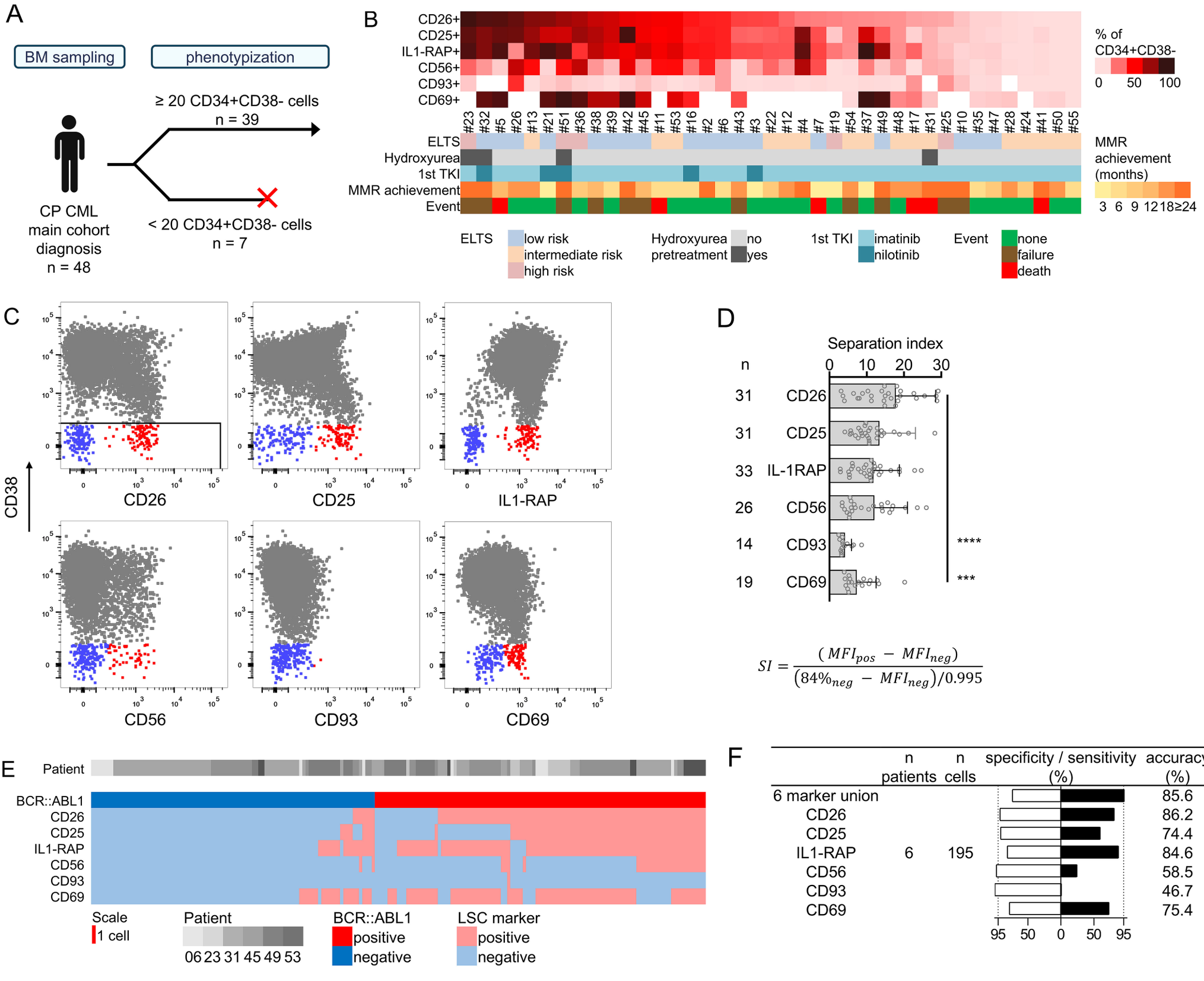
A
BM sampling
phenotypization
≥ 20 CD34+CD38- cells
n = 39
< 20 CD34+CD38- cells
n = 7
CP CML
main cohort
diagnosis
n = 48
B
CD26+
CD25+
IL1-RAP+
CD56+
CD93+
CD69+
% of
CD34+CD38-
0 50 100
#23 #32 #5 #26 #13 #21 #51 #36 #38 #39 #42 #45 #11 #53 #16 #2 #6 #43 #3 #22 #12 #4 #7 #19 #54 #37 #49 #48 #17 #31 #25 #10 #35 #47 #28 #24 #41 #50 #55
ELTS
Hydroxyurea
1st TKI
MMR achievement
Event
MMR
achievement
(months)
3 6 9 12 18 ≥24
ELTS
low risk
intermediate risk
high risk
Hydroxyurea
pretreatment
no
yes
1st TKI
imatinib
nilotinib
Event
none
failure
death
C
CD38
CD26
CD25
IL1-RAP
CD56
CD93
CD69
D
Separation index
n
0 10 20 30
31 CD26
31 CD25
33 IL-1RAP
26 CD56
14 CD93
19 CD69
****
***
$SI = \frac{(MFI_{pos} - MFI_{neg})}{(84\%_{neg} - MFI_{neg})/0.995}$
E
Patient
BCR::ABL1
CD26
CD25
IL1-RAP
CD56
CD93
CD69
Scale
1 cell
Patient
06 23 31 45 49 53
BCR::ABL1
positive
negative
LSC marker
positive
negative
F
n patients
n cells
specificity / sensitivity (%)
accuracy (%)
6 marker union 85.6
CD26 86.2
CD25 74.4
IL1-RAP 6 195 84.6
CD56 58.5
CD93 46.7
CD69 75.4
95 50 0 50 95

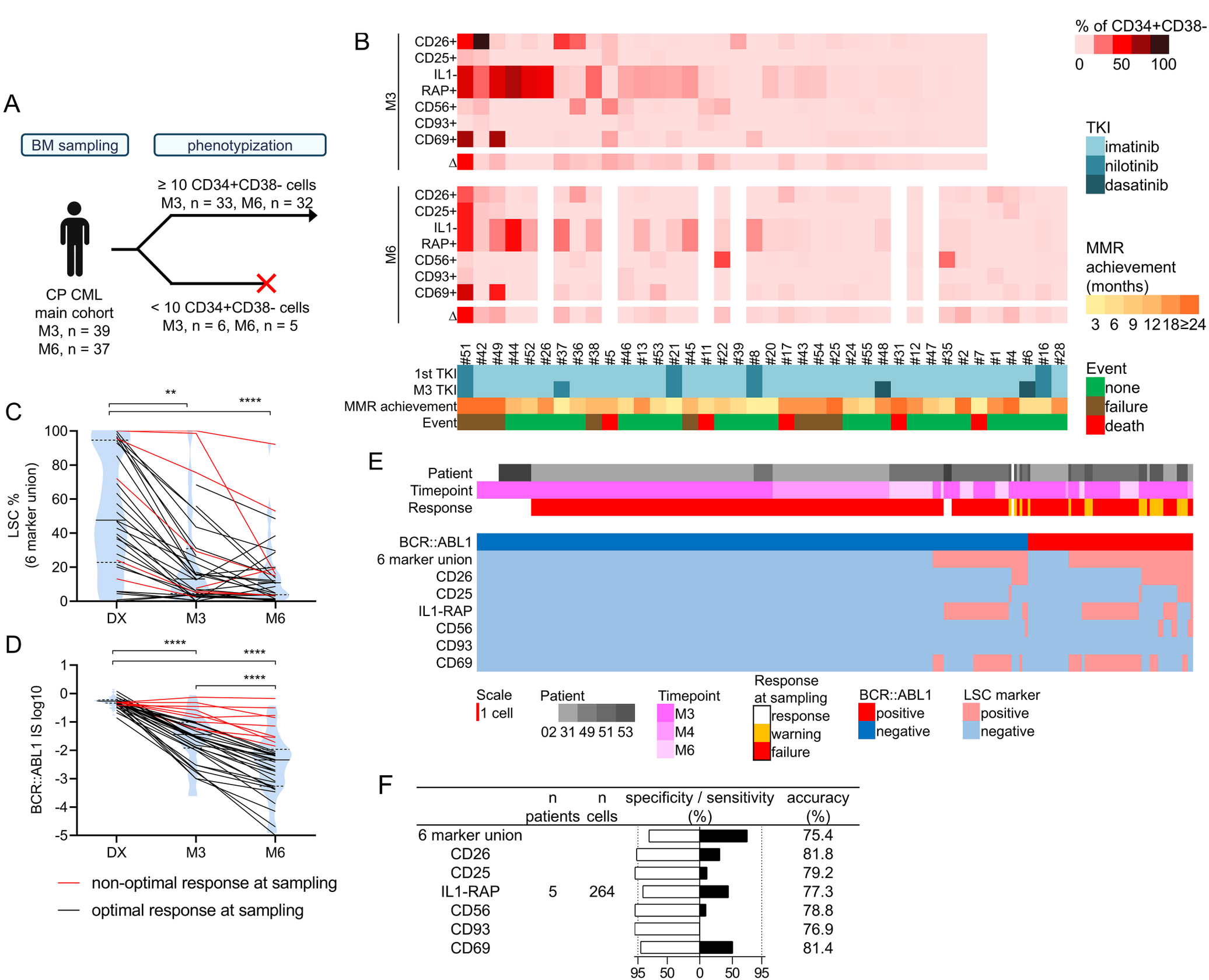
A
BM sampling
phenotypization
≥ 10 CD34+CD38- cells
M3, n = 33, M6, n = 32
CP CML
main cohort
M3, n = 39
M6, n = 37
< 10 CD34+CD38- cells
M3, n = 6, M6, n = 5
B
M3
M6
CD26+
CD25+
IL1-RAP+
CD56+
CD93+
CD69+
Δ
% of CD34+CD38-
0 50 100
TKI
imatinib
nilotinib
dasatinib
MMR achievement (months)
3 6 9 12 18 ≥24
#51 #42 #49 #44 #52 #26 #37 #36 #38 #5 #46 #13 #53 #21 #45 #11 #22 #39 #8 #20 #17 #43 #54 #25 #24 #55 #48 #31 #12 #47 #35 #2 #7 #1 #4 #6 #16 #28
1st TKI
M3 TKI
MMR achievement
Event
Event
none
failure
death
C
LSC % (6 marker union)
DX
M3
M6
**
****
D
BCR::ABL1 IS log10
non-optimal response at sampling
optimal response at sampling
E
Patient
Timepoint
Response
BCR::ABL1
6 marker union
CD26
CD25
IL1-RAP
CD56
CD93
CD69
Scale
1 cell
Patient
02 31 49 51 53
Timepoint
M3
M4
M6
Response at sampling
response
warning
failure
BCR::ABL1
positive
negative
LSC marker
positive
negative
F
n patients
n cells
specificity / sensitivity (%)
accuracy (%)
6 marker union 75.4
CD26 81.8
CD25 79.2
IL1-RAP 5 264 77.3
CD56 78.8
CD93 76.9
CD69 81.4
95 50 0 50 95

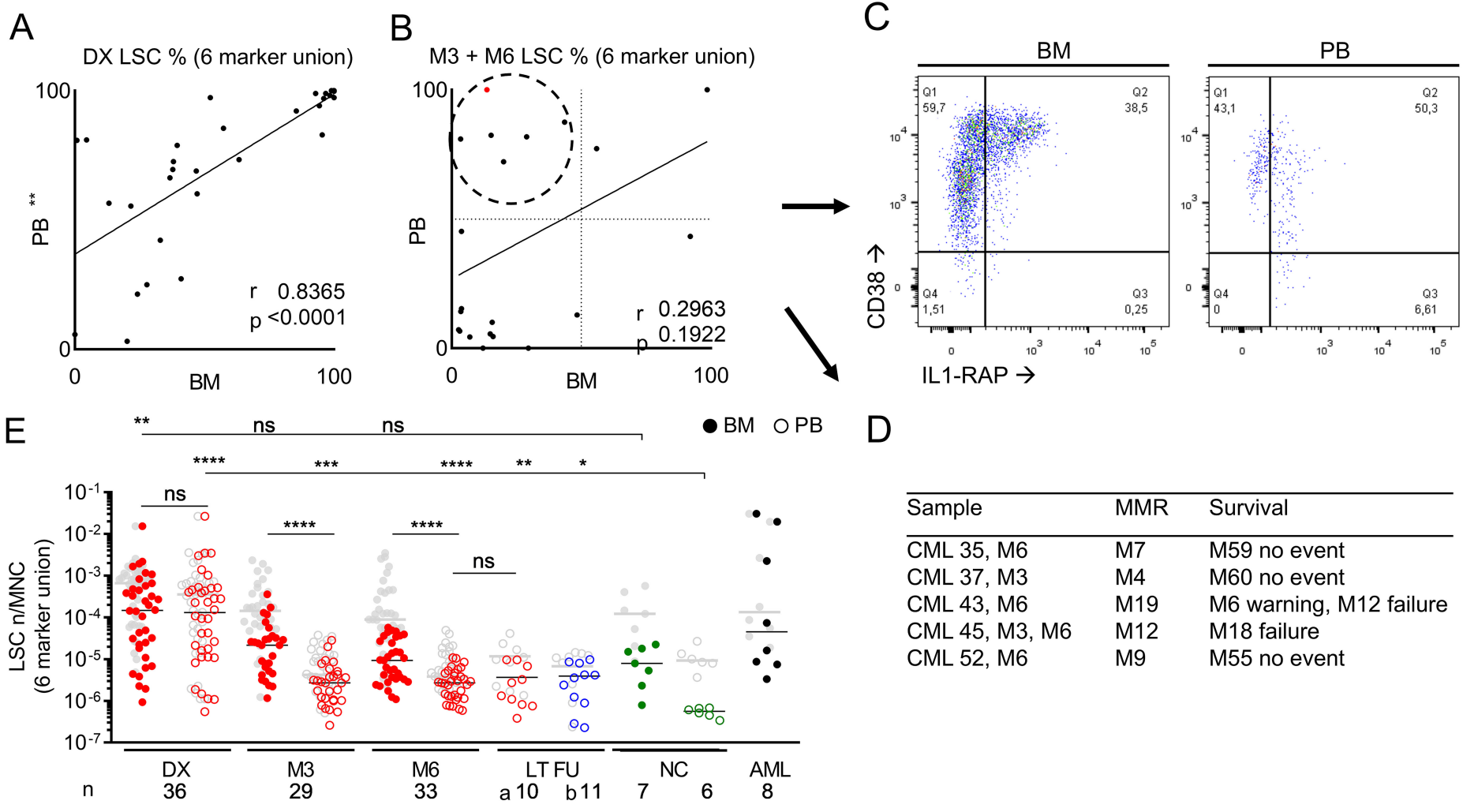
A
DX LSC % (6 marker union)
PB
BM
r 0.8365
p <0.0001
B
M3 + M6 LSC % (6 marker union)
PB
BM
r 0.2963
p 0.1922
C
BM
PB
CD38 →
IL1-RAP →
Q1 59,7
Q2 38,5
Q4 1,51
Q3 0,25
Q1 43,1
Q2 50,3
Q4 0
Q3 6,61
D
Sample | MMR | Survival
CML 35, M6 | M7 | M59 no event
CML 37, M3 | M4 | M60 no event
CML 43, M6 | M19 | M6 warning, M12 failure
CML 45, M3, M6 | M12 | M18 failure
CML 52, M6 | M9 | M55 no event
E
BM PB
LSC n/MNC (6 marker union)
DX M3 M6 LT FU NC AML
n 36 29 33 a 10 b 11 7 6 8

A

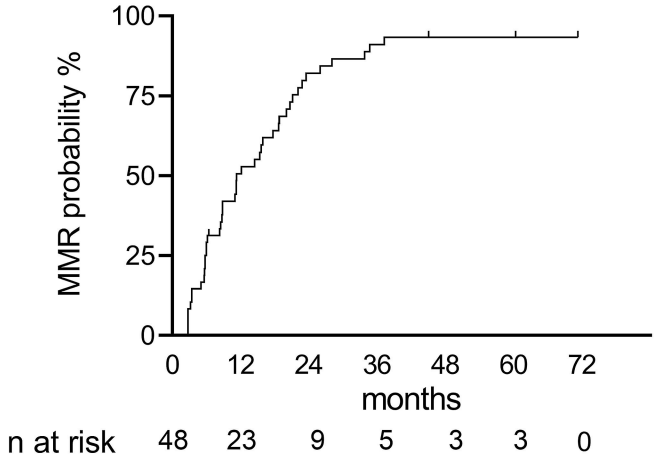

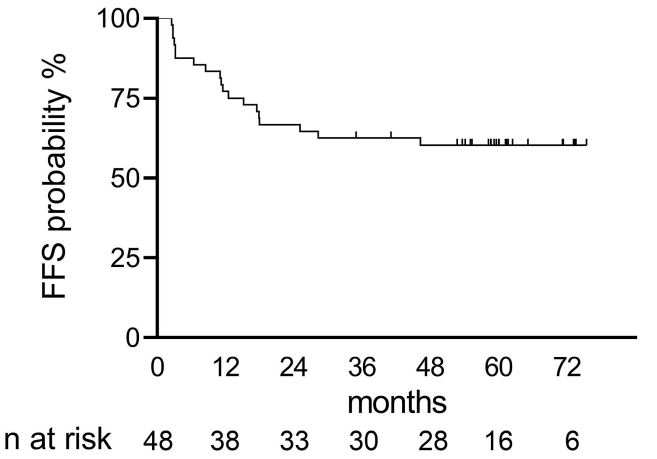

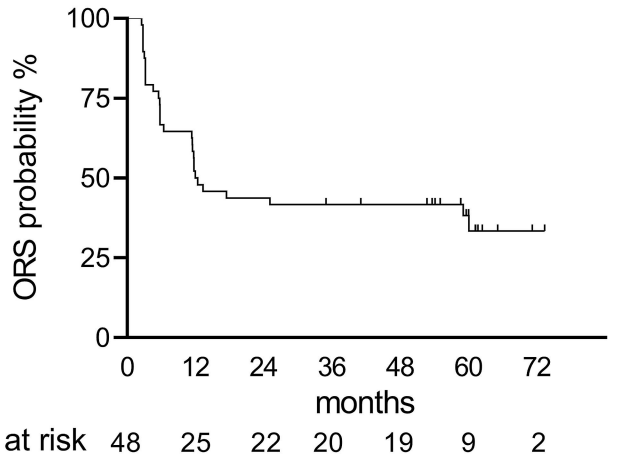

B

Univariate

		MMR	FFS	ORS
DX	LSC %			
	LSC n	6 marker union *		
M3	LSC %	*BCR::ABL1* ***	*BCR::ABL1* ****	*BCR::ABL1* ****
			CD26 * CD69 *	CD25 ** CD69 **
	LSC n	CD26 * CD93 *	CD25 *	
		CD25* CD69 *	CD25* CD93*	
M6	LSC %	*BCR::ABL1* *	*BCR::ABL1* ****	*BCR::ABL1* ****
			CD26 * CD69 *	CD26 * CD69 *
	LSC n			CD25 *

C

Multivariate

		MMR	FFS	ORS
DX	LSC %			
	LSC n			
M3	LSC %		*BCR::ABL1*, CD93 p = 7.00E-09	*BCR::ABL1*, CD25 p = 7.00E-10
	LSC n			
M6	LSC %			*BCR::ABL1*, CD25, CD69 p = 7.00E-10
	LSC n			

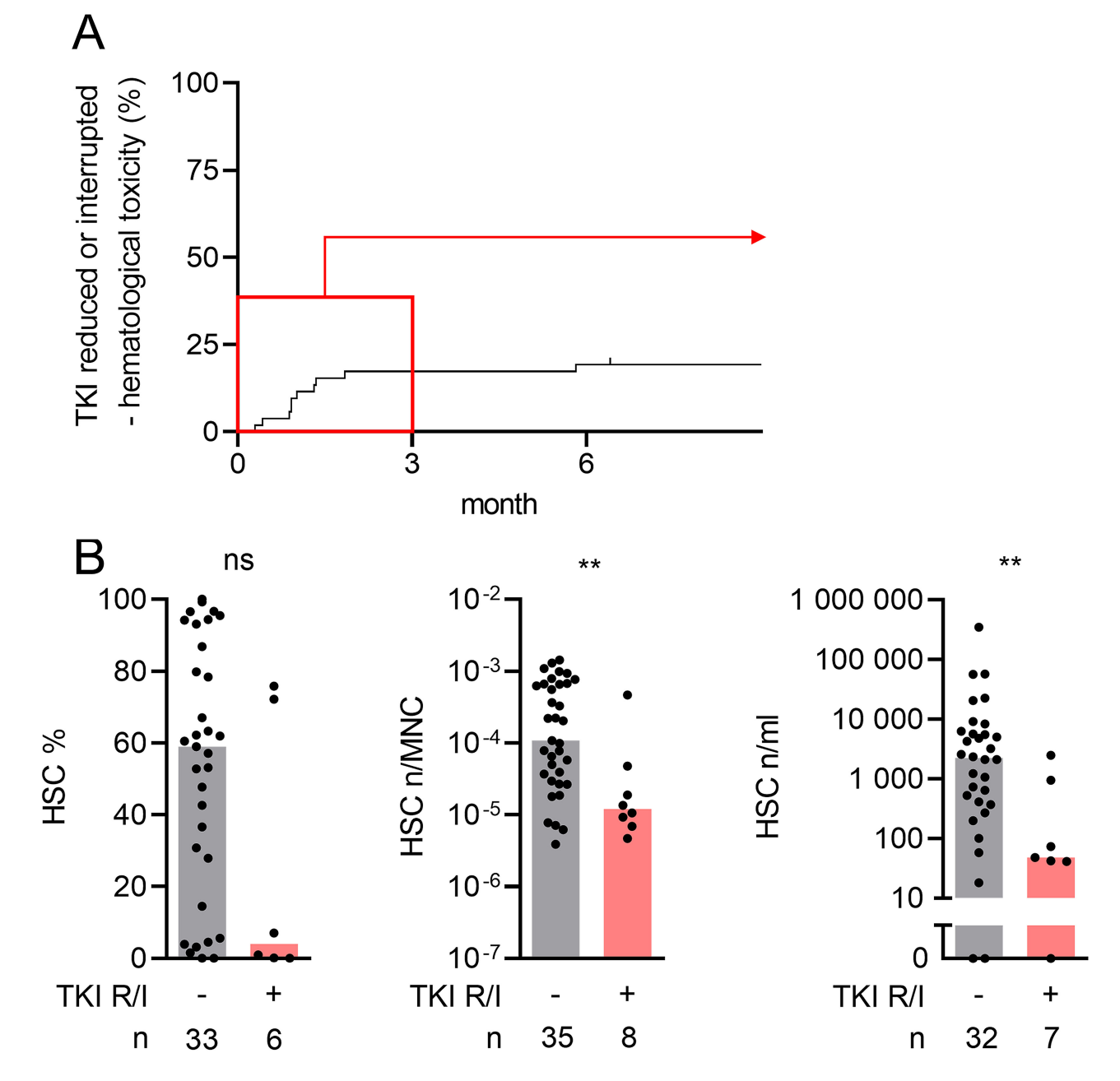
A
TKI reduced or interrupted
- hematological toxicity (%)
100
75
50
25
0
0
3
6
month
B
ns
HSC %
100
80
60
40
20
0
TKI R/I
-
+
n
33
6
**
HSC n/MNC
10-2
10-3
10-4
10-5
10-6
10-7
TKI R/I
-
+
n
35
8
**
HSC n/ml
1 000 000
100 000
10 000
1 000
100
10
0
TKI R/I
-
+
n
32
7

Multicolor detection of chronic myeloid leukemia stem cells, including novel marker CD69, predicts survival and early hematological toxicity

Martin Culen, Marianna Romzova, Dagmar Smitalova, Tomas Loja, Daniel Busa, Ondrej Venglar, Zdenka Herudkova, Samuel Kassa, Lenka Radova, Marek Borsky, Tomas Reigl, Karla Plevova, Jiri Smejkal, Daniela Zackova, Lukas Stejskal, Jiri Mayer

Supplementary Methods, Tables and Figures

Supplementary methods

Flow cytometric leukemic stem cell (LSC) identification and quantification

Samples were processed by erythrocyte-depletion or gradient centrifugation and directly analyzed or cryopreserved (see Table S2). The effect of cryopreservation is described in Figure S15.

Samples were analyzed and sorted on FACSAria IV Fusion (BD Biosciences, USA). Sorting for fluorescence in situ hybridization (FISH) analyses was performed on FACSAria III (BD Biosciences, USA).

RNA gene-expression microarray analysis

RNA was reverse-transcribed and preamplified with Ovation Pico WTA System V2 whole transcriptome amplification kit (NuGEN, USA). Each sample was then fluorescently labelled with SureTag DNA labelling kit (Agilent Technologies, USA) and hybridized on SurePrint G3 human gene expression 8x60k microarray (Agilent Technologies, USA).

Raw microarray data were obtained using Feature extraction software (Agilent Technologies, USA), normalized to the background signal and $\log_2$ transformed. Individual probes' gene expressions were counted as medians in each population.

To validate microarray results by PCR, reverse transcription of RNA samples was performed using Superscript VILO Master Mix (Thermo Fisher Scientific, USA). The relative expression of selected genes was measured on SmartChip real-time PCR system (Takara Bio, Kusatsu, Japan) with KAPA SYBR fast qPCR master mix (Merck, Germany) and custom-made primers (Generi Biotech, Czech Republic).

***BCR::ABL1* single-cell analysis**

Single cells were sorted into 4 μl of lysis buffer (0.2% Triton X100 with 2U/μl RNase inhibitor) in a 96 well-plate.

The *BCR::ABL1* analysis was initially performed using in house protocol 1) and later, protocol 2) was adopted.

Protocol 1: Reverse transcription using SuperScript VILO MasterMix (Thermo Fisher Scientific, USA) was followed by targeted preamplification using *BCR::ABL1* primers from EAC protocol[1] and KAPA SYBR FAST qPCR Master Mix (2X) Kit (Merck, Germany). The product with KAPA SYBR FAST qPCR Master Mix (2X) Kit (Merck, Germany) was analyzed on a SmartChip Real-Time PCR System (Takara Bio, USA) and data

analyzed in the SmartChip Real-Time PCR System's software.

Protocol 2: Single cell libraries and subsequent single cell *BCR::ABL1* detection were performed as described by Giustacchini et al.[2] Quantitative PCR was performed on the QuantStudio 12-Flex Real-Time PCR System (Thermo Fisher Scientific, USA) and data analyzed in the QuantStudio 12-Flex Real-Time PCR System's software.

No clear difference was found between the performance of the two protocols (Figure S27).

FISH

Cells were sorted into an approximately 20 µl drop of saline, confined within a circle drawn with a hydrophobic pen on polylysine-coated glass slides. After 30 min sedimentation at 4°C, the slide was immersed into a fixative solution of methanol-acetic acid (3: v/v) and dried at room temperature.

Detecting *BCR::ABL1* fusion was performed on interphase nuclei using the XL BCR/ABL1 plus probe (MetaSystems, Germany). Hybridization followed the manufacturer's recommendations with modifications: 7 µl of probe mixture was applied per slide; washes included 4 min in 0.4X SSC / 0.3% NP-40 solution (Abbott Molecular, USA) at 73.5°C, followed by 2 min in 2X SSC / 0.1% NP-40 solution (Abbott Molecular, USA) at room temperature. Fluorescence signals were evaluated using a Nikon Eclipse E80i fluorescence microscope and documented with LUCIA FISH software (Laboratory Imaging, Czech Republic).

References

1. Gabert J, Beillard E, van der Velden VH, et al. Standardization and quality control studies of “real-time” quantitative reverse transcriptase polymerase chain reaction of fusion gene transcripts for residual disease detection in leukemia - a Europe Against Cancer program. Leukemia 2003;17(12):2318–57.

2. Giustacchini A, Thongjuea S, Barkas N, et al. Single-cell transcriptomics uncovers distinct molecular signatures of stem cells in chronic myeloid leukemia. Nat Med 2017;23(6):692–702.

Supplementary tables

Table S1. Summary of patient and donor characteristics.

Chronic phase chronic myeloid leukemia patients		
Age	(years; median, range)	59, 18-82
Gender	(count; female/male)	33/37
Additional cytogenetic abnormalities	(count; yes/no/not available)	4/53/13
ELTS classification	(count; low/intermediate/high)	34/24/12
1st line tyrosine kinase inhibitor	(count; imatinib/nilotinib/bosutinib/not applicable)	57/11/1/1
Normal controls, bone marrow		
Age years	(years; median, range)	55, 21-71
Gender	(count; female/male)	4/3
Normal controls, peripheral blood		
Age	(years; median, range)	47, 44-57
Gender	(count; female/male)	6/0

* ELTS – EUTOS long-term survival score.

Table S2. Detailed patient and donor characteristics. Table shows individual i) characteristics of patients and donors, at individual sampling points, ii) flow cytometry results, and iii) clinical outcomes used for prognostication. The table is divided into sections, respecting the individual paragraphs in the main text and their order of appearance. Some patients/samples were used in multiple analyses/paragraphs and are therefore listed multiple times in different sections of the table (e.g., patient 2 – is listed in sections B, D, E, F, G, H, I, K). The table is included as a separate excel file.

Table S3. Antibody list.

Antigen	Fluorochrome	Maker	Clone
7AAD	647 nm	Invitrogen	-
CD45	APC-Cy7	SONY	Hi30
CD34	FITC	SONY	581
CD38	PE-Cy7	SONY	HB-7
CD26	PE-CF594	SONY	M-A261
CD25	BV786	SONY	M-A251
IL-1RAP	APC	Miltenyi	REA558
CD56	BV711	SONY	NCAM
CD90	BV421	SONY	Thy1
CD93	PE	SONY	VIMD2
CD69	BV605	SONY	FN50
CD32	PE	SONY	FUN-2
CD36	BV786	SONY	5-271
CD85d	APC	SONY	ILT4
CD185	BV605	SONY	J252D4
CD206	BV711	SONY	MMR
CD370	BV421	SONY	CLEC9A/DNGR1

Table S4. qPCR validation of selected deregulated/potentially deregulated genes from microarray analysis.

	LSCs vs HSCs				progenitors vs HSCs						
	microarray		qPCR		microarray			qPCR			
gene	log2 fold change	p	log2 fold change	p	log2 fold change	adj p	p	log2 fold change	p	systematic name	Full name	NCBI role
CBX7	-2.06	0.019	-2.49	0.001	-4.24	0.050	0.000	-4.84	0.002	NM_175709	chromobox 7	component of the Polycomb repressive complex 1 (PRC1); thought to control the lifespan of several normal human cells
CDK6	1.24	0.016	-0.19	0.231						NM_001259	cyclin dependent kinase 6	catalytic subunit of the protein kinase complex that is important for cell cycle G1 phase progression and G1/S transition
GSK3B	1.67	0.015	-0.53	0.008						NM_002093	glycogen synthase kinase 3 beta	negative regulator of glucose homeostasis; involved in energy metabolism, inflammation, ER-stress, mitochondrial dysfunction, and apoptotic pathways
IGJ	3.07	0.002	4.36	0.001						NM_144646	joining chain of multimeric IgA and IgM	enables IgA binding activity and protein homodimerization activity; contributes to several functions including immunoglobulin receptor binding activity, peptidoglycan binding activity, and phosphatidylcholine binding activity
IRF2	1.74	0.009	-0.55	0.003						NM_002199	interferon regulatory factor 2	competitively inhibits the IRF1-mediated transcriptional activation of interferons alpha and beta, and presumably other genes that employ IRF1 for transcription activation
MAPKAPK3	1.38	0.018	0.02	0.674						NM_004635	MAPK activated protein kinase 3	shown to be activated by growth inducers and stress stimulation of cells
MYB	-1.30	0.005	-1.24	0.000						NM_005375	MYB proto-oncogene, transcription factor	transcription regulator, essential role in the regulation of hematopoiesis, may be aberrantly expressed or rearranged or undergo translocation in leukemias and lymphomas and is considered to be an oncogene
MYCBP2	-1.66	0.001	-0.85	0.001	-1.76	0.063	0.000	-1.53	0.001	NM_015057	MYC binding protein 2	regulates the cAMP and mTOR signaling pathways, and may additionally regulate autophagy, reduced expression of this gene has been observed in acute lymphoblastic leukemia patients
PCNA	1.54	0.020	0.33	0.191						NM_002592	proliferating cell nuclear antigen	increases the processivity of leading strand synthesis during DNA replication, is ubiquitinated In response to DNA damage and is involved in the RAD6-dependent DNA repair pathway
PELI2	-2.09	0.001	-0.91	0.002						NM_021255	pellino E3 ubiquitin protein ligase family member 2	predicted to enable protein-macromolecule adaptor activity and ubiquitin protein ligase activity
PIK3C3	1.44	0.007	-0.37	0.013						NM_002647	phosphatidylinositol 3-kinase catalytic subunit type 3	autophagy and positive regulation of protein lipidation
RAD51	1.81	0.003	1.14	0.017						NM_002875	RAD51 recombinase	involved in the homologous recombination and repair of DNA
RALA	1.08	0.021	0.70	0.001	-1.05	0.195	0.025	-0.88	0.001	NM_005402	RAS like proto-oncogene A	ras-like GTP-binding protein
RFC4	1.17	0.000	0.02	0.985						NM_002916	replication factor C subunit 4	required for elongation of primed DNA templates by DNA polymerase delta and DNA polymerase epsilon
RSU1	2.02	0.001	-0.11	0.865						NM_012425	RAS suppressor protein 1	involved in the Ras signal transduction pathway, growth inhibition, and nerve-growth factor induced differentiation processes
STMN1	1.53	0.011	0.62	0.025	1.76	0.120	0.005	1.07	0.009	NM_203401	stathmin 1	regulation of the microtubule filament system by destabilizing microtubules
TAB2	-1.13	0.013	-1.26	0.002	-1.65	0.131	0.008	-2.55	0.001	NM_015093	TGF-beta activated kinase 1 (MAP3K7) binding protein 2	activator of MAP3K7/TAK1, which is required for the IL-1 induced activation of nuclear factor kappaB and MAPK8/JNK
TIMELESS	1.74	0.001	1.07	0.012	1.26	0.135	0.008	1.43	0.010	NM_003920	timeless circadian regulator	cell survival after damage or stress, increase in DNA polymerase epsilon activity, maintenance of telomere length, and epithelial cell morphogenesis
TPM2	-1.18	0.102	-0.89	0.027	-3.64	0.085	0.002	-4.02	0.001	NM_001301 226	tropomyosin 2	actin filament binding protein family, and mainly expressed in slow, type 1 muscle fibers
TRIB1	2.44	0.012	-0.23	0.844						NM_025195	tribbles pseudokinase 1	involved in several processes, including JNK cascade; negative regulation of lipopolysaccharide-mediated signaling pathway; and regulation of protein kinase activity
TUBA8	1.34	0.027	-2.55	0.001						NM_018943	tubulin alpha 8	heterodimerizes with beta tubulin and assembles to form microtubules
HDC					2.73	0.061	0.000	2.88	0.031	NM_002112	histidine decarboxylase	forms a homodimer that converts L-histidine to histamine in a pyridoxal phosphate dependent manner
IGF1R					-2.42	0.152	0.012	-3.13	0.001	NM_000875	Fc gamma receptor Ia	plays an important role in the immune response, a high-affinity Fc-gamma receptor
MPC2					2.26	0.033	0.000	1.78	0.001	NM_015415	mitochondrial pyruvate carrier 2	involved in mitochondrial pyruvate transmembrane transport

* adj p – adjusted p, HSCs – normal hematopoietic stem cells, LSCs – leukemic stem cells.

Table S5. Additional information about the most deregulated surface marker genes from microarray analysis.

marker	NCBI role	role in CML	source 1	source 2
CD36	thrombospondin receptor, involved in fatty acid transport	CD36 defines a subpopulation of primitive CML cells with decreased imatinib sensitivity; CD36+ LSCs protected by adipose tissue in mouse models	Landberg	Ye
CD370	group V C-type lectin-like receptor, myeloid lineage cells, activation receptor	NA (expressed on cDC1 dendritic cells)	Harada	
CD25	part of IL2 receptor, regulation of immune tolerance by controlling Tregs	expression on CML LSCs, negative growth regulator of CML LSCs	Sadovnik	
CD32	cell surface receptor found on phagocytic cells such as macrophages and neutrophils; involved in the process of phagocytosis and clearing of immune complexes	CD32 expressed on CML and AML LSCs; also expressed on normal BM	Warfvinge	
CD233	anion exchange transporter, structural protein, in erythrocytes	under-expressed in AML	Dalman	
CD206	mannose receptor, endocytosis of glycoproteins by macrophages, phagocytosis	macrophage marker, significantly higher in BM of CML patients	Song	
CD85D	binds to major histocompatibility complex class I molecules on antigen-presenting cells and transduces a negative signal that inhibits stimulation of an immune response; controls inflammatory responses and cytotoxicity to help focus the immune response and limit autoreactivity	CLL-specific biomarker, highly expressed on AML cells	Hodges	
CD26	cleaves X-proline dipeptides from the N-terminus of polypeptides; involved in glucose and insulin metabolism, as well as in immune regulation	specific marker of CML LSCs; successfully targeted with chimeric antigen receptor (CAR) macrophages	Herrmann	Guoyun
CD225	restricts cellular entry by diverse viral pathogens, such as influenza A virus, Ebola virus and Sars-CoV-2	higher *IFITM1* expression correlated with improved survival in CML patients; elevated in *BCR::ABL1* positive stem cells	Akyerli	Giustacchini
CD36L2	lysosomes and endosomes, membrane transportation and the reorganization of endosomal/lysosomal compartment	NA (scavenger protein, hepatocellular carcinoma, infections)	Wang	
CD69	induced upon activation of T lymphocytes, and may play a role in proliferation. Furthermore, the protein may act to transmit signals in natural killer cells and platelets.	1. CD69 expression directly upregulated by BCR::ABL1; 2. CD69 partially inhibits apoptosis and erythroid differentiation via CD24	Hantschel	Huang
CD62L	binding and subsequent rolling of leucocytes on endothelial cells, facilitating their migration into secondary lymphoid organs and inflammation sites	expression of CD62L was significantly lower in CML patients than in normal controls; BCR::ABL1 dependent	Fruehauf	
CD110	megakaryocytopoiesis, platelet formation	high expression on human HSC, mutated in myeloproliferative neoplasms	Ninos	
CD209	cell adhesion and pathogen recognition	NA (expressed on dendritic cells)		
CD164	proliferation, adhesion and migration of hematopoietic progenitor cells, interaction with the C-X-C chemokine receptor type 4	highly expressed by primitive hematopoietic progenitor cells	Watt	
CD117	important role in hematopoiesis, stem cell maintenance, gametogenesis, melanogenesis, and in mast cell development, migration and function	low c-KIT levels in primitive, quiescent, drug-resistant leukemia-initiating CML cells	Shah	
CD185	expressed in mature B-cells and Burkitt's lymphoma, binds to B-lymphocyte chemoattractant, and is involved in B-cell migration into B-cell follicles of spleen and Peyer patches	overexpression in B-CLL	Bürkle	
CD42C	part of the GPIb-V-IX system that constitutes the receptor for von Willebrand factor, and mediates platelet adhesion in the arterial circulation	NA (expressed on platelets)		

* AML – acute myeloid leukemia, CLL – chronic lymphocytic leukemia, CML – chronic myeloid leukemia, HSC – normal hematopoietic stem cell, LSC – leukemic stem cell, NA – not available.

Supplementary figures

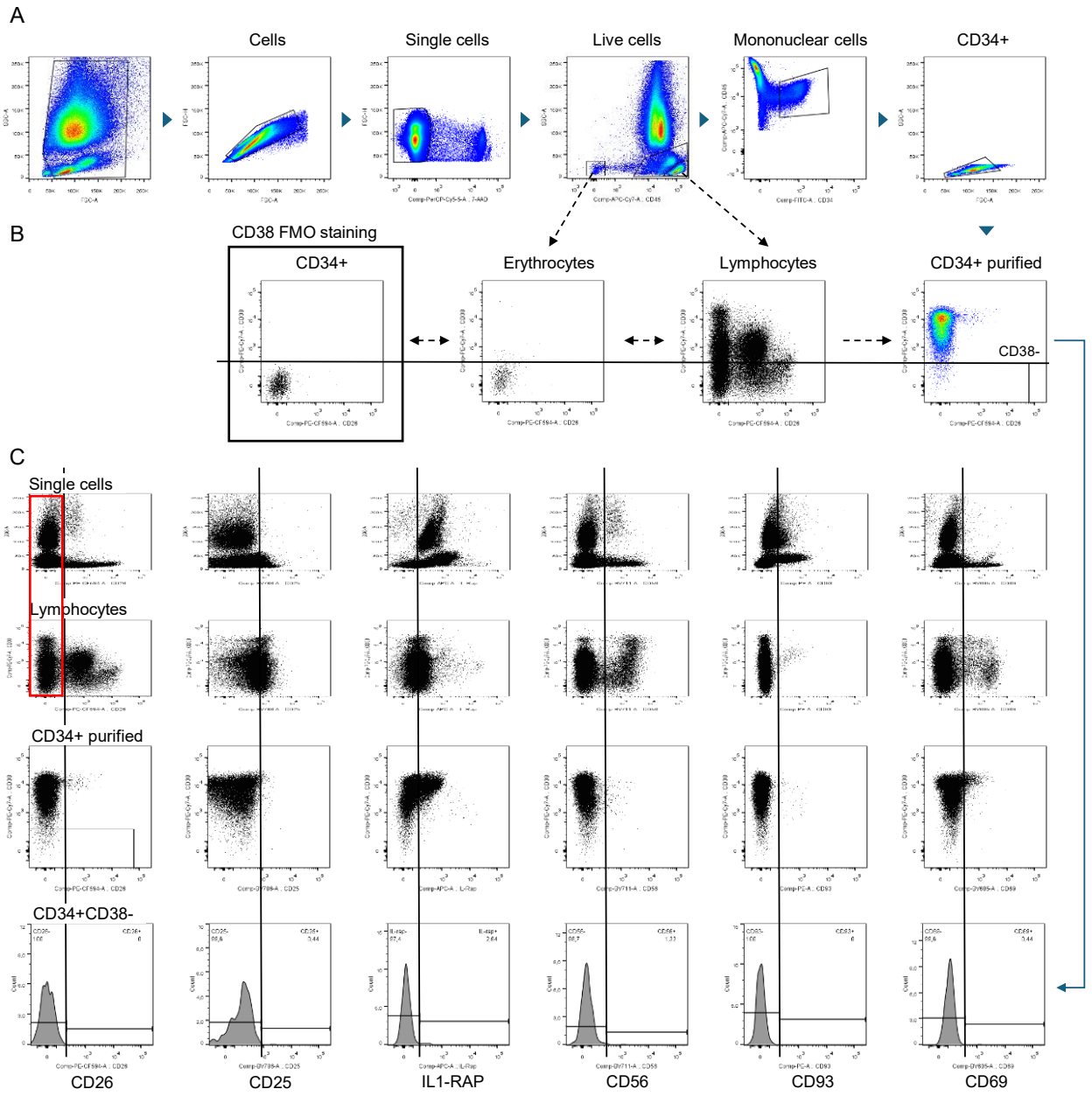

Figure S1. Gating strategy, demonstrated on a normal bone marrow control sample BM NC1. A – Basic gates shown consecutively. B – CD38- gating. Since CD38 negativity may vary with different antibody, instrument, staining concentration or time, the following controls were established to ensure identical CD38- gating between experiments and different sample types (left to right): 1) CD38 fluorescence minus one (FMO) control was prepared by staining an additional tube of the same sample with all antibodies except CD38. The FMO was influenced by cryopreservation and CD38 antibody (data not shown) and was used for orientation only. 2) Erythrocyte remnants (not always present) and 3) lymphocytes served as "internal controls" from the analyzed sample. The lymphocyte control was preferred. C – Gating of LSC markers. A set of internal controls was used. The CD34+ purified fraction was always visualized and helped orientation. Gating was set according to lymphocytes and granulocytes (red rectangle).

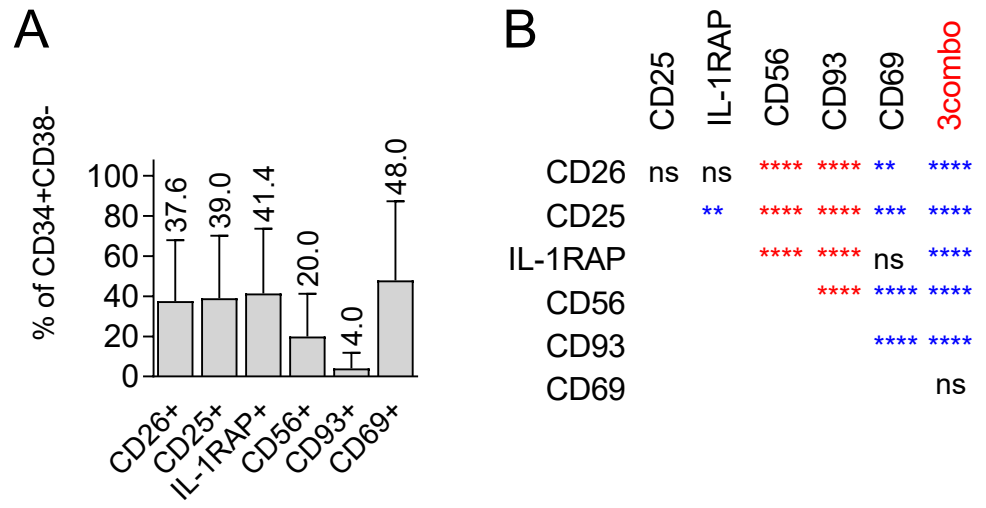

Figure S2. Comparison of LSC markers at diagnosis in bone marrow (data from Figure 2B). A – Percentage of positive cells according to different markers in the CD34+CD38- fraction, mean ± SD. B – Statistical comparison of the results from (A). Non-parametric one-way ANOVA. LSC – leukemic stem cell, ns – not significant. ** $p < 0.0$ **** $p < 0.0001$ The blue color indicates less and red more LSCs identified by the marker in the row.

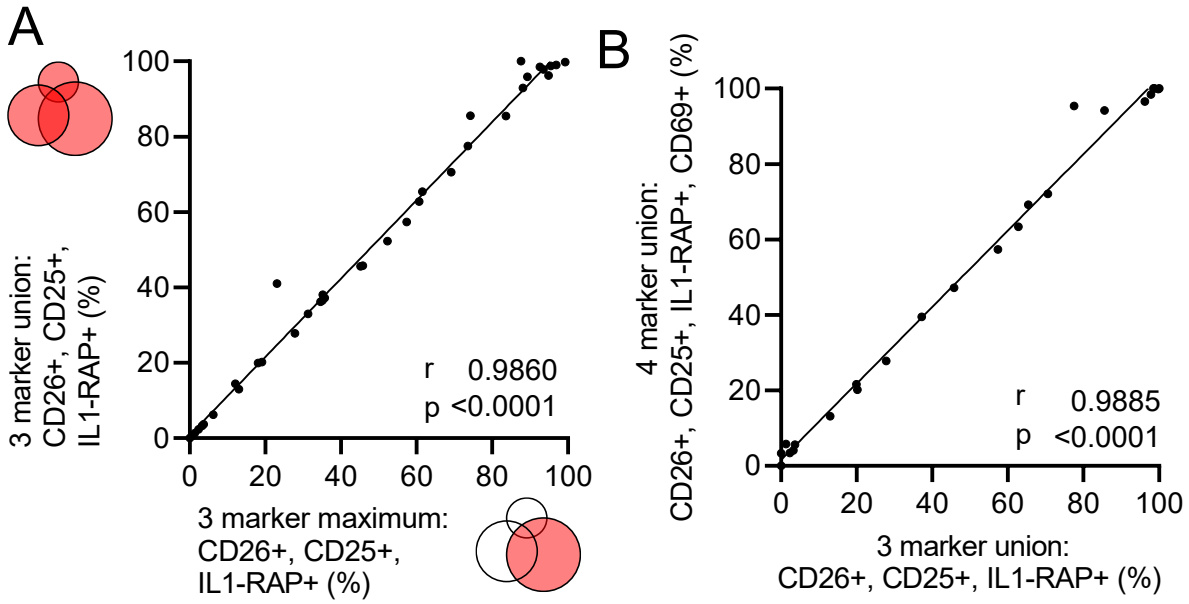

Figure S3. Comparison of LSC markers in bone marrow at CML diagnosis. A – Analysis of expression overlap for CD26, CD25, IL1-RAP, n = 39. The marker with the highest positivity correlated with the union (OR gate) of all 3 markers. Shown as % of CD34+CD38-. Spearman correlation. B – Analysis of expression overlap for CD69 vs. CD26, CD25, and IL1-RAP, n = 24. Correlation of the CD26, CD25, IL1-RAP union with and without CD69. Shown as % of CD34+CD38-. Spearman correlation. CML – chronic myeloid leukemia, LSC – leukemic stem cell.

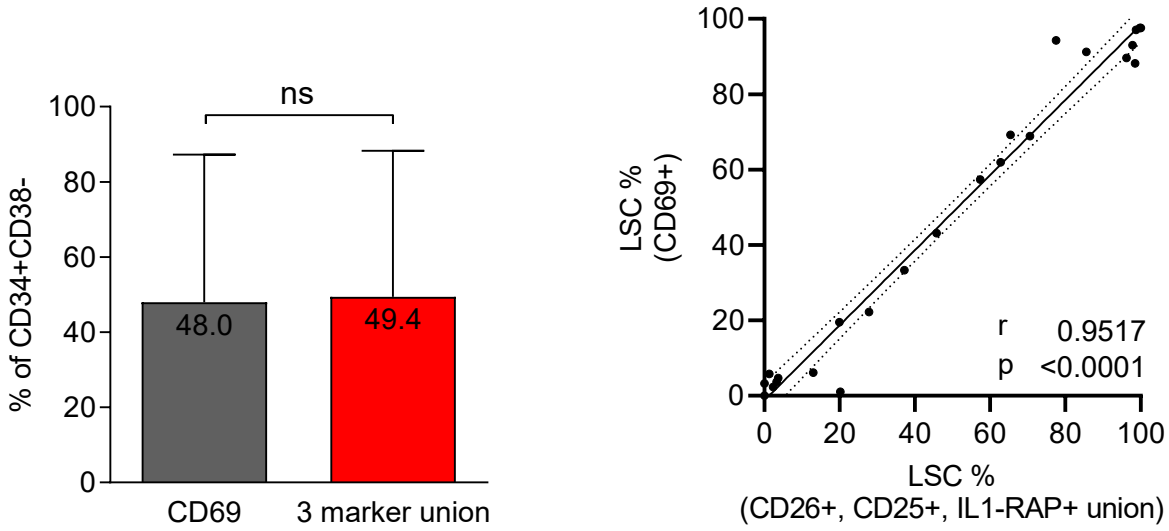

Figure S4. LSC detection at diagnosis in bone marrow by CD69 vs 3 marker union (CD26+ or CD25+ or IL1-RAP+). Wilcoxon non-parametric, unpaired t-test, Spearman correlation. LSC – leukemic stem cell, ns – not significant.

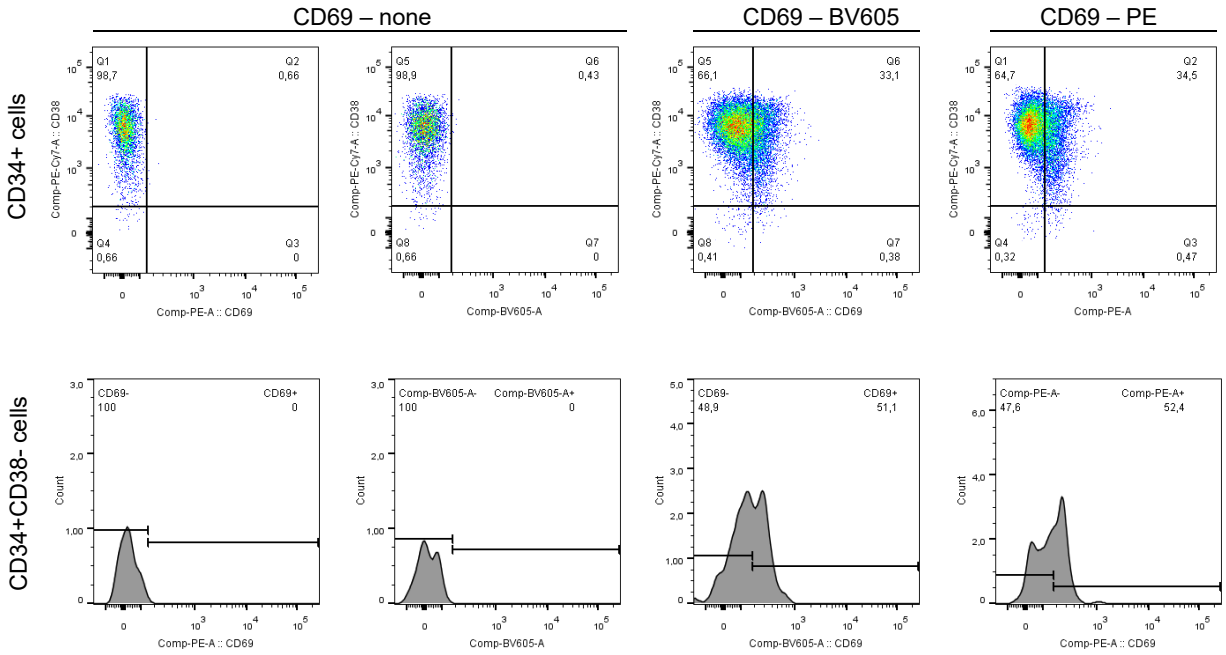

Figure S5. Testing of alternative CD69 clone CH/4 in PE (Invitrogen, USA) vs. the standard clone FN50 in BV605 (SONY, USA). Sample CML 45, diagnosis, bone marrow.

sample ID	n cells	specificity / sensitivity (%)	accuracy (%)
F1	186		38.2
F2	176		82.7
F3	59		78.0
F4	150		94.0
F5	413		68.3
mean			**72.2**

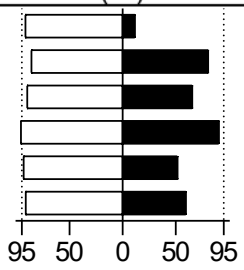

Figure S6. Assessment of CD69 specificity in Fluorescence-Activated Cell Sorting isolated cells using fluorescence in-situ hybridization. Five bone marrow samples from diagnosis were analyzed. n – number; ID – patient identifier.

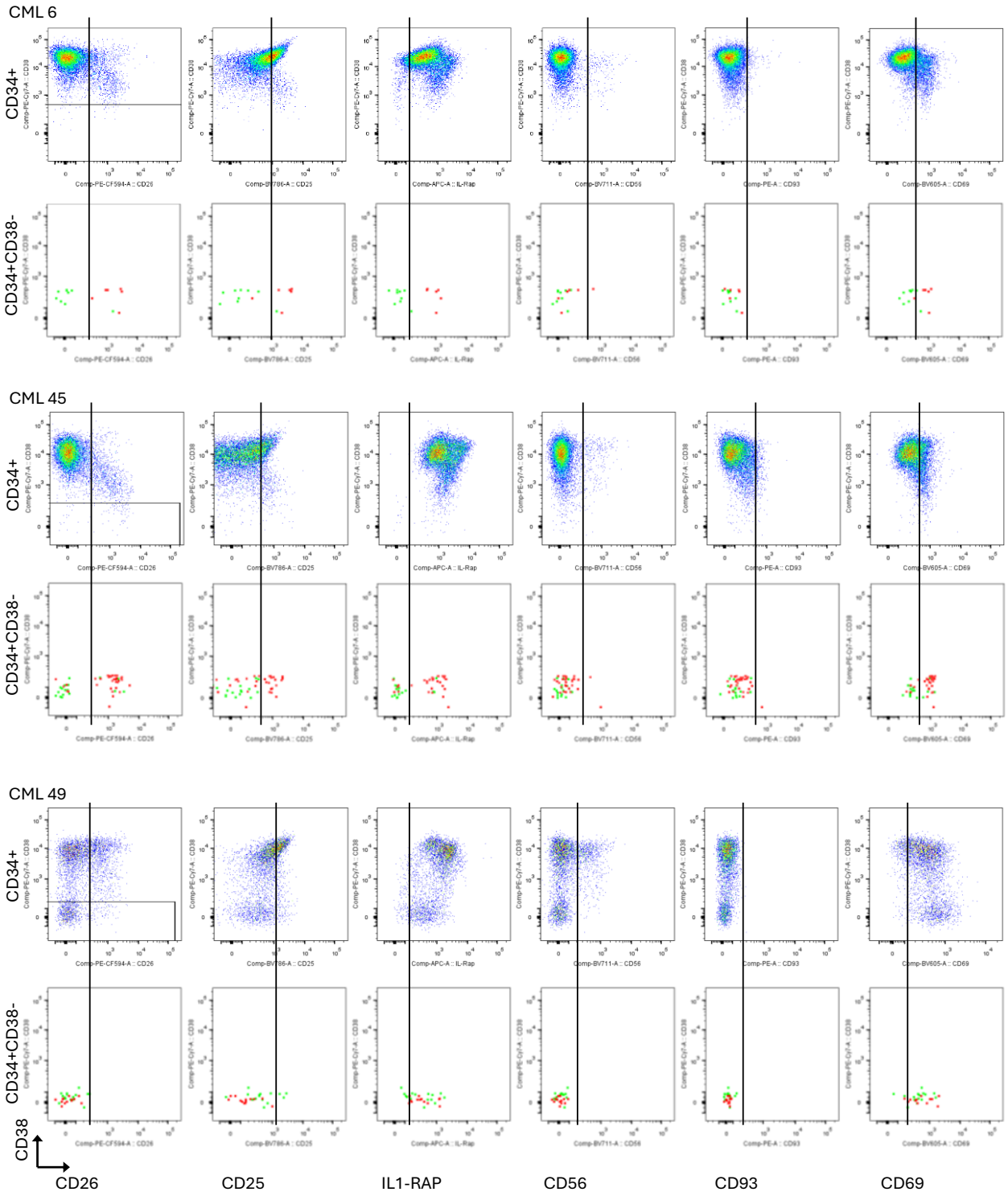

Figure S7. Depiction of *BCR::ABL1* positive cells in dotplots at diagnosis. Single cells from bone marrow were index sorted on a 96 well-plate and the *BCR::ABL1* positivity was analyzed at RNA level by qPCR analysis. Three representative bone marrow samples were chosen to demonstrate different match between LSC marker and *BCR::ABL1* expression, from good match in CML 6 (top) to poor match in CML 49 (bottom). For each sample, upper row shows bulk sample phenotypization (CD38- gating shown on the

left), and the bottom row shows dot-plots from single cell index sorting of CD34+CD38- cells, with color-coded *BCR::ABL1* status (green = *BCR::ABL1*^{neg}, red = *BCR::ABL1*^{pos}). LSC marker gating is indicated by vertical lines. LSC – leukemic stem cell.

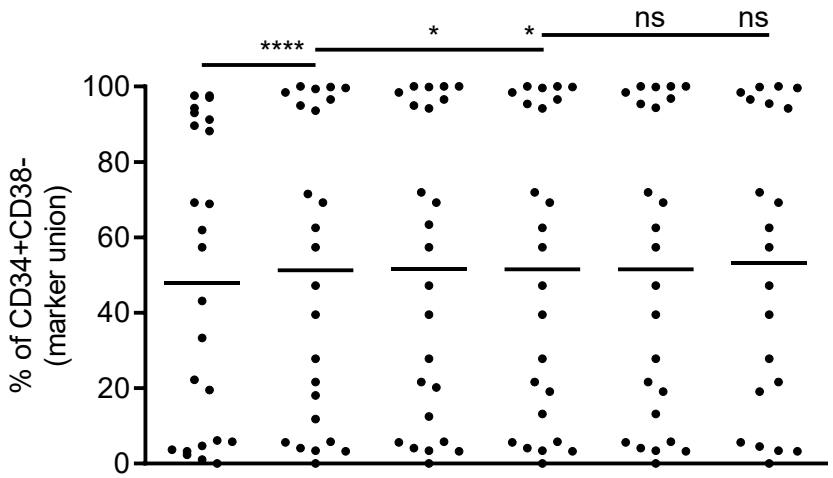

n	24					21
CD69	+	+	+	+	+	+
IL1-RAP		+	+	+	+	+
CD25			+			
CD26				+	+	+
CD56					+	
CD93						+

Figure S8. Determining minimum combination of markers required for robust LSC detection in bone marrow at CML diagnosis. Only samples with CD69 analyzed included, 3/24 without CD93. Mean, paired, non-parametric t-test. CML – chronic myeloid leukemia, LSC – leukemic stem cell, n – number/count, ns – not significant. * $p < 0.05$, **** $p < 0.0001$.

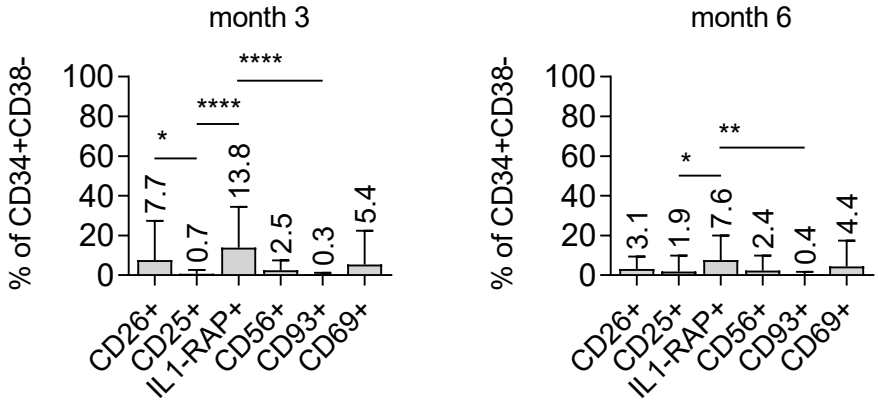

Figure S9. Comparison of LSC markers in BM at M3 and M6 after starting TKI treatment (data summary from Figure 3B). Percentage of positive cells according to different markers in the CD34+CD38- fraction, mean ± SD. Non-parametric one-way ANOVA, only statistically significant results shown. BM – bone marrow, LSC – leukemic stem cell, M – month, TKI – tyrosin kinase inhibitor.* $p < 0.05$, ** $p < 0.0$ **** $p < 0.0001$.

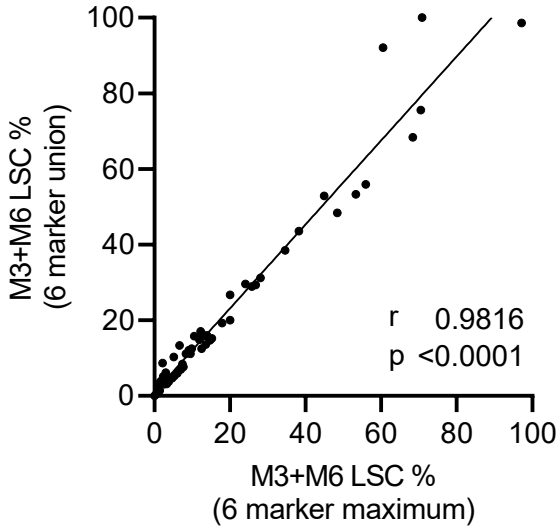

Figure S10. Comparison of LSC markers at M3 and M6 in BM after starting TKI treatment. Analysis of expression overlap. Marker with the highest positivity correlated with union (OR gate) of all markers. Shown as % of CD34+CD38- cells, 65 M3 + M6 samples. Linear regression and Spearman correlation. BM – bone marrow, LSC – leukemic stem cell, M – month, TKI – tyrosin kinase inhibitor.

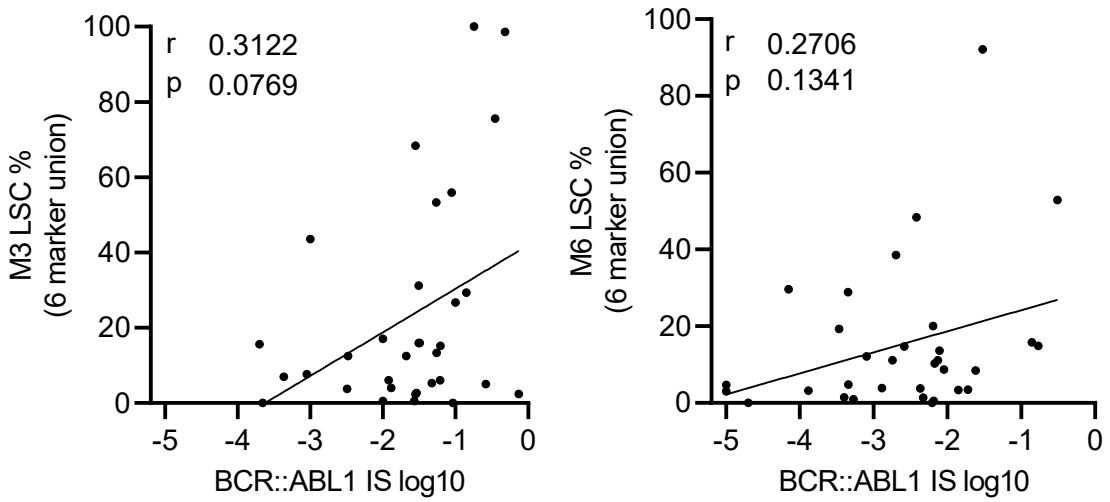

Figure S11 Correlation of BM LSC % vs. bulk *BCR::ABL1* transcript levels in 65 M3 or M6 samples. Linear regression and Spearman correlation. BM – bone marrow, IS – international scale, LSC – leukemic stem cell, M – month.

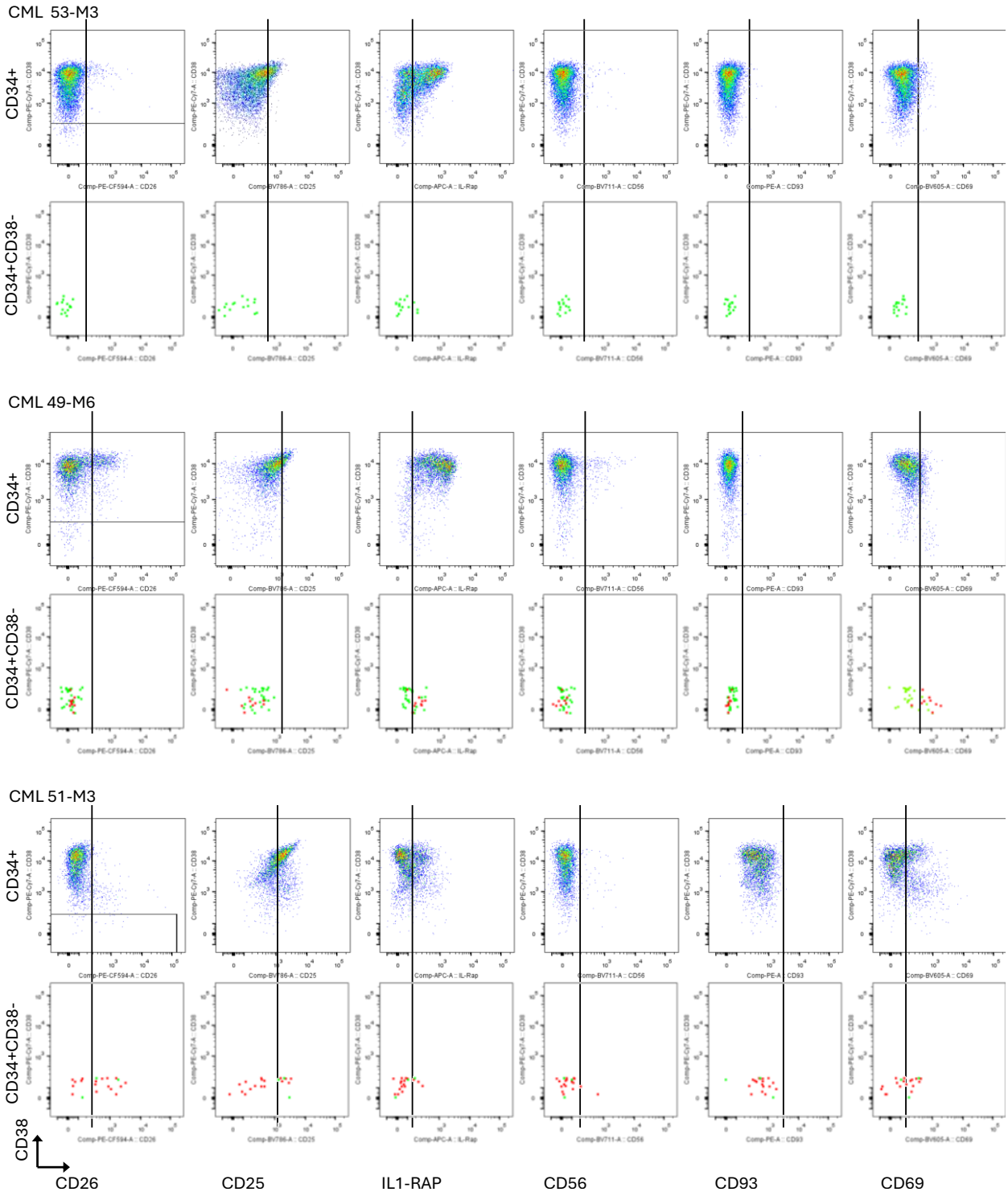

Figure S12. Depiction of *BCR::ABL1* positive cells in dotplots at month 3 or 6. Single cells from bone marrow were index sorted on a 96 well-plate and the *BCR::ABL1* positivity was analyzed at RNA level by qPCR analysis. Three representative samples were chosen. CML 53 from month 3 represents a sample with matching *BCR::ABL1*^{neg} and LSC marker negative cells. CML 49 at month 6 demonstrates a sample with LSCs lacking expression on most markers, except IL1-RAP and CD69. CML 51 at month 3 again shows

a sample where the individual LSC markers identify only a subset of the *BCR::ABL1*^{pos} cells, but union/OR gate identifies 16/17 (94%) LSCs. For each sample, upper row shows bulk sample phenotypization (CD38- gating shown on the left), and the bottom row shows dot-plots from single cell index sorting of CD34+CD38- cells, with color-coded *BCR::ABL1* status (green = *BCR::ABL1*^{neg}, red = *BCR::ABL1*^{pos}). LSC marker gating is indicated by vertical lines. LSC – leukemic stem cell.

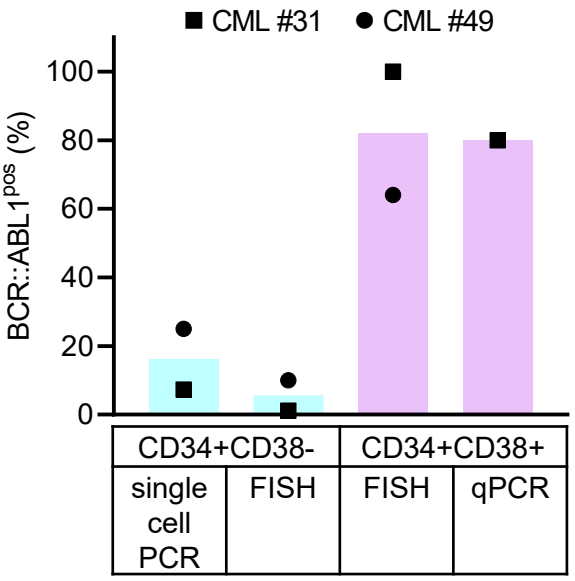

Figure S13. *BCR::ABL1* positivity in bone marrow stem vs. progenitor cells at treatment failure. CML 31 analyzed at month 4 without complete hematological response and 57% IS *BCR::ABL1* transcript level in peripheral blood. CML 49 analyzed at month 6 with minimal cytogenetic response and 31% IS *BCR::ABL1* transcript level in peripheral blood.

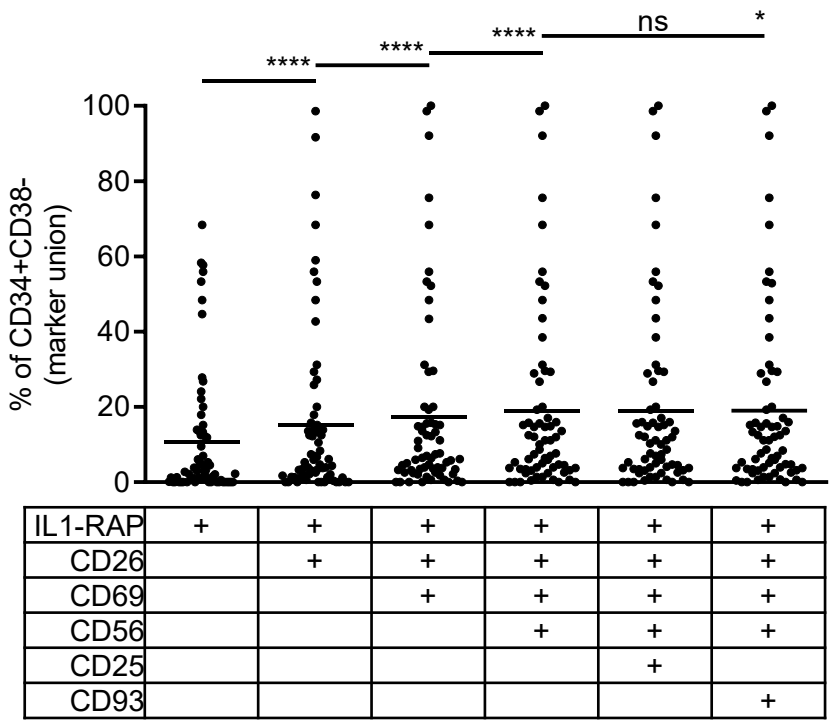

Figure S14. Comparison of LSC markers in bone marrow at M3 and M6 after starting TKI treatment. Determining the minimum combination of markers required for robust LSC detection, 65 M3 or M6 samples. Mean, paired, non-parametric t-test. LSC – leukemic stem cell, M – month, ns – not significant. * $p < 0.05$, **** $p < 0.0001$.

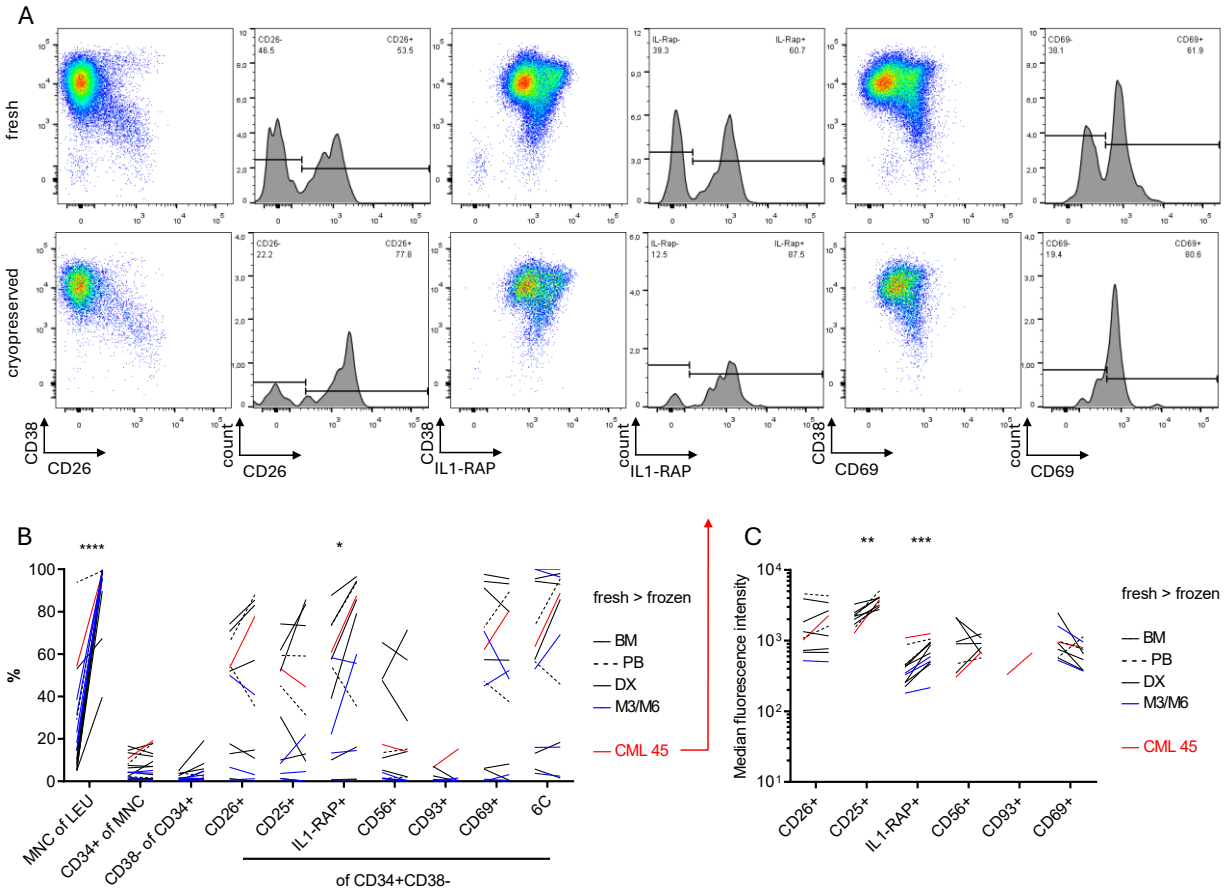

Figure S15. The effect of cryopreservation examined in 13 fresh-cryopreserved sample pairs. A – Example of LSC marker expression shown on CML 45 DX BM. B – Quantitative comparison. Cryopreservation led to the concentration of the MNC fraction due to granulocyte death but did not alter the frequency of CD34+ and CD34+CD38- fractions. For LSC markers, the percentage of LSCs within the CD34+CD38- fraction exhibited an increase or decrease from 0 to 40%. Statistically significant shift was observed only for IL1-RAP. Some samples, for example the one shown in (A), showed a higher ratio of LSCs post cryopreservation across multiple markers. C – Qualitative comparison of LSC marker expression revealed minimal yet statistically significant qualitative changes for CD25 and IL1-RAP. As seen in (A), these changes did not affect the overall population distribution or impair the gating strategy. B, C – 13 pairs analyzed: 9 DX BM, 3 DX PB, 3 M3 BM, 2 M6 BM. Paired, non-parametric t-test. Only statistically significant values shown. 6C – six LSC marker union, BM – bone marrow, DX – diagnosis, M – month of follow-up, MNC – mononuclear cells, PB – peripheral blood. * $p < 0.05$, ** $p < 0.0$ *** $p < 0.00$ **** $p < 0.0001$.

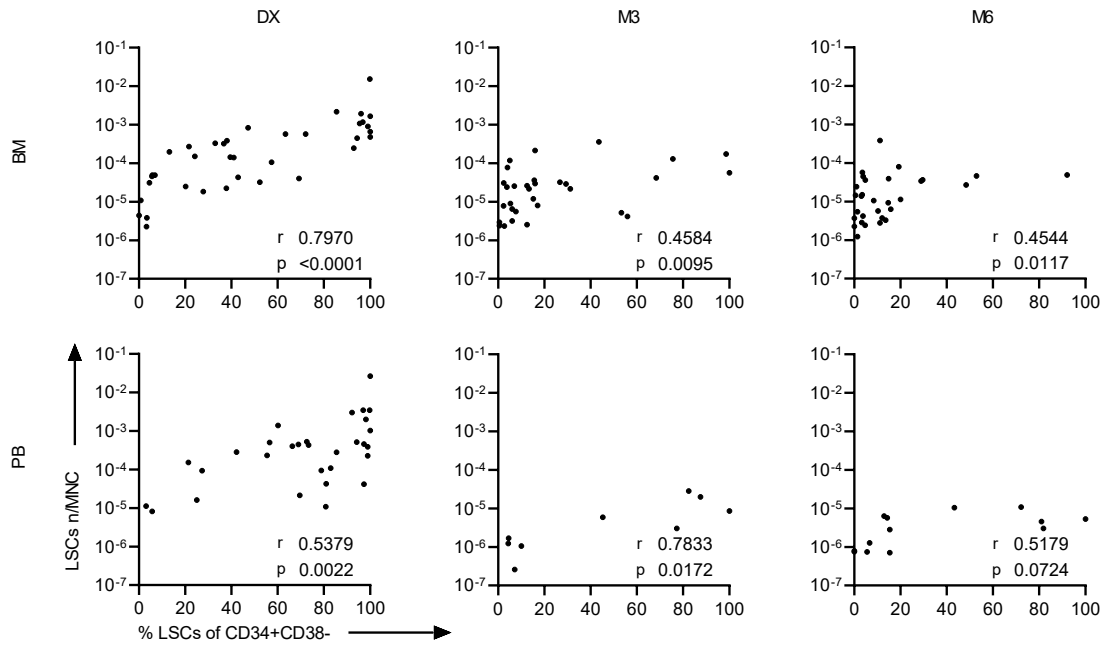

Figure S16. Correlation of two LSC metrics, LSC % vs. LSC n/MNC. Spearman correlation. BM – bone marrow, DX – diagnosis, LSC – leukemic stem cell, M – month, MNC – mononuclear cell, n – number, PB – peripheral blood.

LSC n/MNC BCR::ABL1	DX BM	DX PB	M3 BM	M3 BM M3 PB	M3 PB	M6 BM	M6 BM M6 PB	M6 PB	LT FU a+b PB
r	0.3441	0.5491	0.2744	0.3076	0.1423	0.1429	0.1600	0.2174	-0.1799
p	**0.0319**	**0.0004**	0.1286	0.0767	0.4222	0.4128	0.3587	0.1898	0.4351

Figure S17. Correlation of LSC n/MNC (BM or PB) with bulk *BCR::ABL1* transcript levels (BM or PB). Spearman correlation. BM – bone marrow, DX – diagnosis, LSC – leukemic stem cell, M – month, MNC – mononuclear cells, PB – peripheral blood.

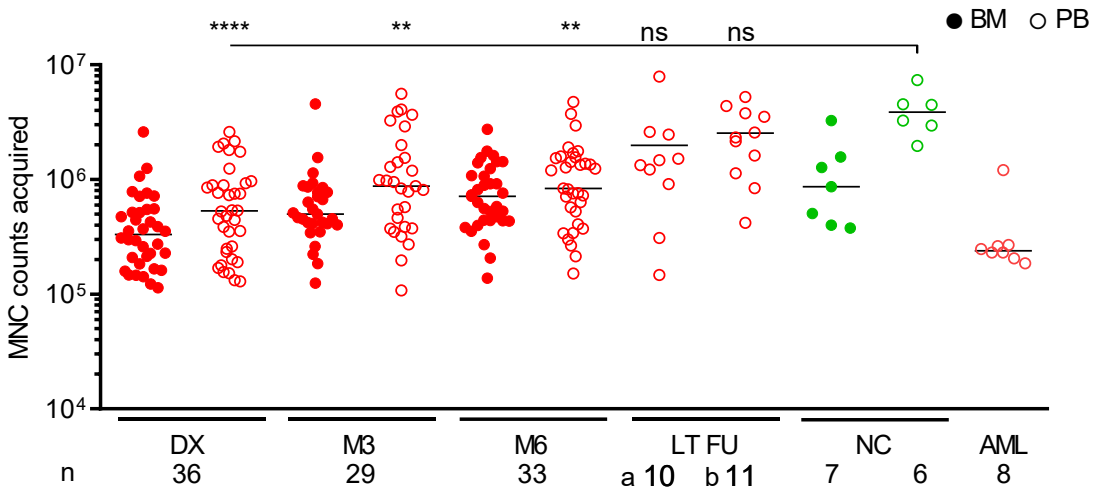

Figure S18. MNC counts from Figure 4E. Only samples/pairs with 100k MNCs included. DX, M3, M6: matched BM-PB pairs, patients from the main cohort. LT FU a: main cohort patients, year 2-5 from diagnosis, 7/10 in MMR at sampling. LT FU b: additional CP CML patients with 2-10 year long MMR or better. NC: PB and BM from non-matched donors. AML: acute myeloid leukemia samples from diagnosis. BM – bone marrow, CML – chronic phase chronic myeloid leukemia, DX – diagnosis, M – month, MMR – major molecular response, MNC – mononuclear cells, NC – normal control, ns – not significant, PB – peripheral blood. ** $p < 0.0$ **** $p < 0.0001$

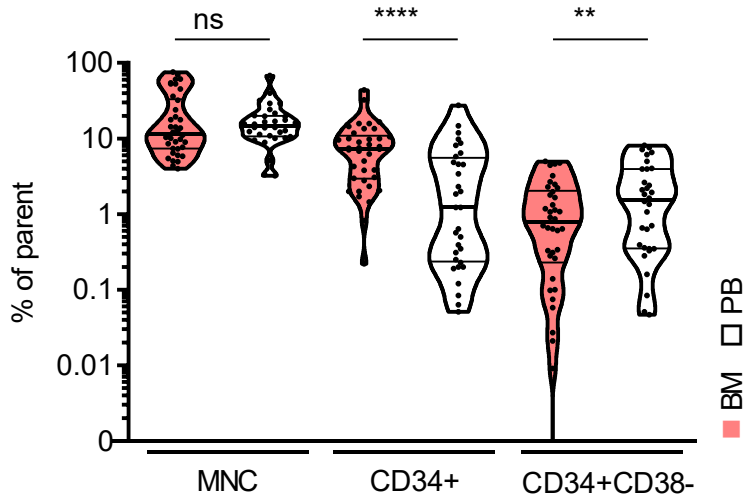

Figure S19. Distribution of hierarchically ordered cell fractions in BM and PB at diagnosis. MNC fraction of all leukocytes, CD34+ of MNC, CD34+CD38- of CD34+. Fresh, matched DX BM-PB samples from 32 main cohort CP CMLs. Median with interquartile range, non-parametric, paired t-test. BM – bone marrow, CP CML – chronic phase chronic myeloid leukemia, MNC – mononuclear cells, ns – not significant, PB – peripheral blood. ** $p < 0.0$ **** $p < 0.0001$.

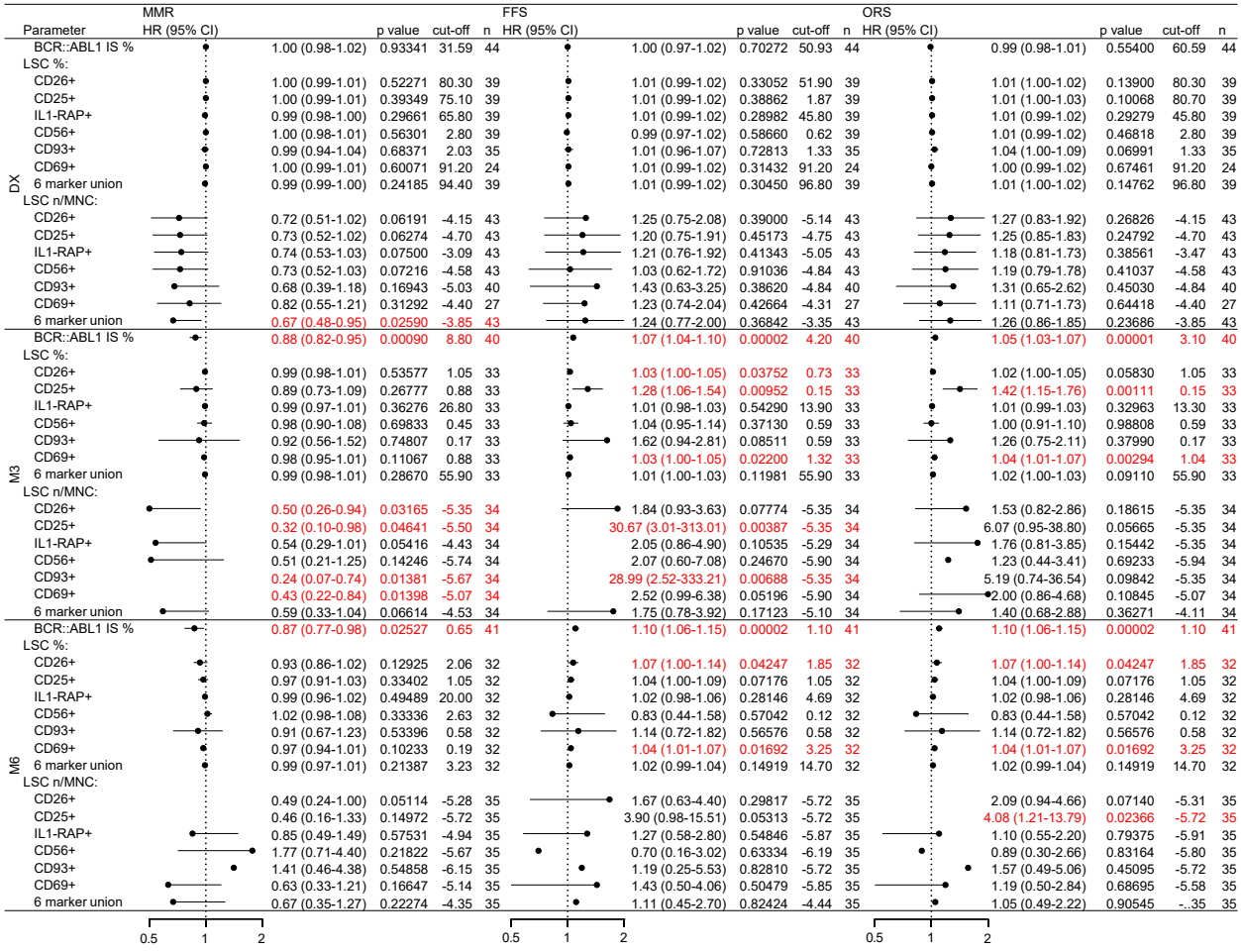

Figure S20. Prognostic value of BM LSC data. Univariate Cox models of LSC data for MMR, FFS, and ORS at DX, M3, and M6. LSC data shown both as % of LSCs from CD34+CD38- fraction (LSC %) or number of LSCs from MNC fraction (LSC n/MNC). LSC identification performed based on individual markers or the 6 marker union (positivity for any marker). *BCR::ABL1* transcript levels from PB included as a positive control. Red values denote statistical significance. BM – bone marrow. CI – confidence interval. DX – diagnosis. FFS – failure-free survival. HR – hazard ratio. IS – international scale. LSC – leukemic stem cell. M – month. MMR – cumulative major molecular response. n – number. ORS – optimum response survival.

A

		MMR					FFS						ORS					
		parameter	coefficient	HR	95% CI (min-max)	p value	logrank P	parameter	coefficient	HR	95% CI (min-max)	p value	logrank P	parameter	coefficient	HR	95% CI (min-max)	p value	logrank P
DX	LSC %			NA						NA						NA			
	LSC n			NA						NA						NA			
M3	LSC %			NA				BCR::ABL1	0.06670	1.07	1.03 1.11	0.00008	7.00E-09	BCR::ABL1	0.05751	1.06	1.03 1.09	0.00006	7.00E-10
								CD93+	0.61850	1.86	1.04 3.33	0.03780		CD25+	0.36037	1.43	1.14 1.80	0.00196	
	LSC n			NA						NA						NA			
M6	LSC %			NA						NA				BCR::ABL1	0.20120	1.22	1.10 1.35	0.00011	3.00E-07
														CD25+	0.17110	1.19	1.06 1.32	0.00235	
														CD69+	-0.08281	0.92	0.86 0.99	0.01871	
	LSC n			NA						NA						NA			

B

		AIC
FFS – M3	BCR-ABL and CD93+	57,72
	BCR-ABL	55,8
ORS – M3	BCR-ABL and CD25+	99,5
	BCR-ABL	100,89
ORS – M6	BCR-ABL and CD25+ and CD69+	96,61
	BCR-ABL	100,89

C

		Brier score				
		1year	2years	3years	4years	5years
FFS – M3	BCR-ABL and CD93+	0,0679	0,1382	0,1564	0,1567	0,1569
	BCR-ABL	0,066	0,1405	0,1581	0,1583	0,1593
ORS – M3	BCR-ABL and CD25+	0,1785	0,1997	0,2041	0,2041	0,2032
	BCR-ABL	0,1934	0,2102	0,2132	0,2133	0,2129
ORS – M6	BCR-ABL and CD25+ and CD69+	0,1634	0,1796	0,1821	0,1833	0,1881
	BCR-ABL	0,1933	0,2102	0,2132	0,2133	0,2129

Figure S21. Prognostic value of BM LSC data; multivariate analysis. A – The best multivariate Cox regression models of BM LSC data correlated with MMR, FFS, and ORS at DX, M3, M6. LSC data shown both as % of LSCs from CD34+CD38- fraction (LSC %) or the number of LSCs from MNC fraction (LSC n). B – Evaluation of the best multivariate models using AIC (Akaike information criteria; left). A lower AIC indicates a better fitting model. C – Evaluation of the best multivariate models using Brier score. Brier score signifies more accurate predictions. Particular years of follow-up (1-5) evaluated separately. General: Red values denote differences between the evaluated models. *BCR::ABL1* transcript levels from PB are shown as international scale %. BM – bone marrow. CI – confidence interval. HR – hazard ratio. IS – international scale. FFS – failure-free survival. LSC – leukemic stem cell. M – month. MMR – cumulative major molecular response. ORS – optimum response survival. PB – peripheral blood.

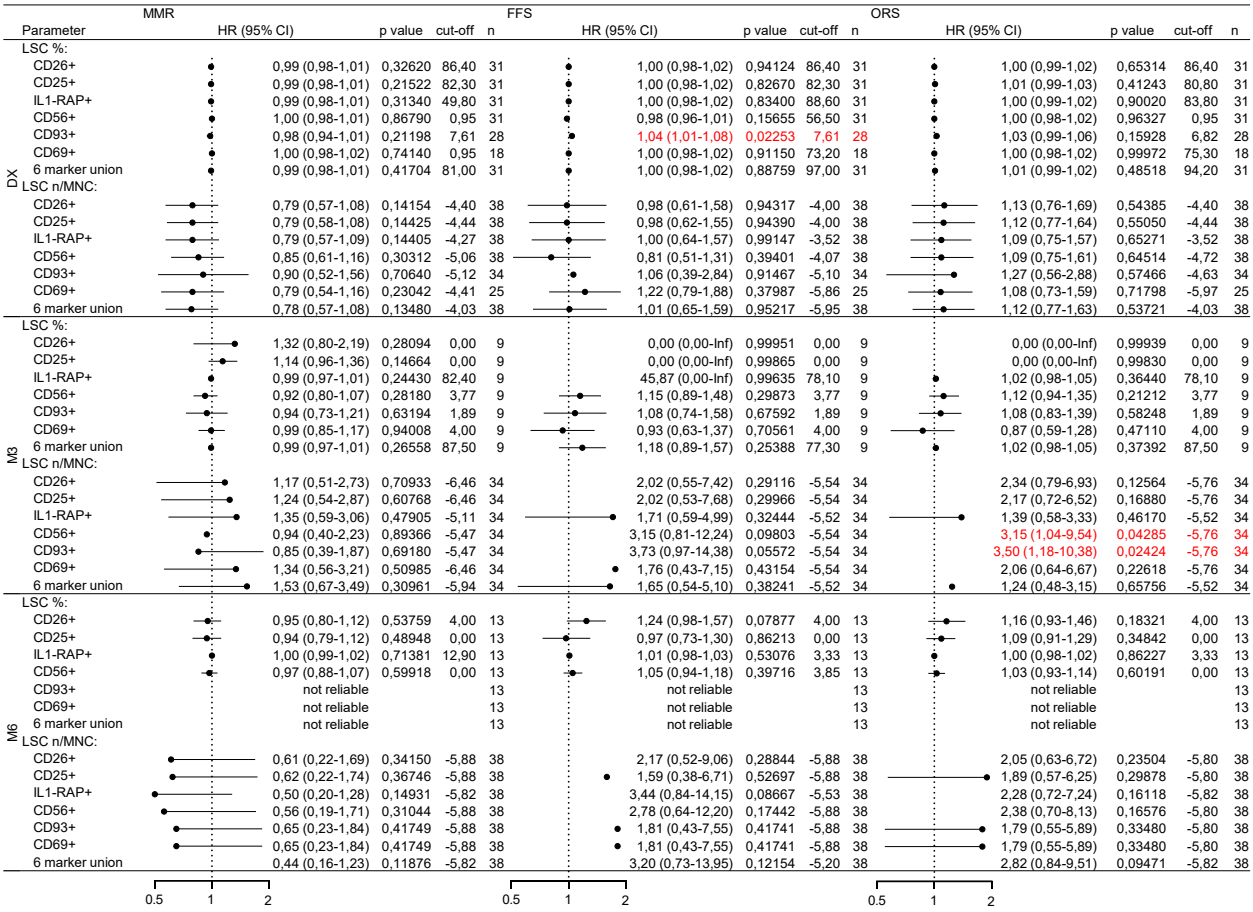

	Parameter	MMR HR (95% CI)	MMR p value	MMR cut-off	MMR n	FFS HR (95% CI)	FFS p value	FFS cut-off	FFS n	ORS HR (95% CI)	ORS p value	ORS cut-off	ORS n
DX	LSC %:												
	CD26+	0,99 (0,98-1,01)	0,32620	86,40	31	1,00 (0,98-1,02)	0,94124	86,40	31	1,00 (0,99-1,02)	0,65314	86,40	31
	CD25+	0,99 (0,98-1,01)	0,21522	82,30	31	1,00 (0,98-1,02)	0,82670	82,30	31	1,01 (0,99-1,03)	0,41243	80,80	31
	IL1-RAP+	0,99 (0,98-1,01)	0,31340	49,80	31	1,00 (0,98-1,02)	0,83400	88,60	31	1,00 (0,99-1,02)	0,90020	83,80	31
	CD56+	1,00 (0,98-1,01)	0,86790	0,95	31	0,98 (0,96-1,01)	0,15655	56,50	31	1,00 (0,98-1,02)	0,96327	0,95	31
	CD93+	0,98 (0,94-1,01)	0,21198	7,61	28	1,04 (1,01-1,08)	0,02253	7,61	28	1,03 (0,99-1,06)	0,15928	6,82	28
	CD69+	1,00 (0,98-1,02)	0,74140	0,95	18	1,00 (0,98-1,02)	0,91150	73,20	18	1,00 (0,98-1,02)	0,99972	75,30	18
	6 marker union	0,99 (0,98-1,01)	0,41704	81,00	31	1,00 (0,98-1,02)	0,88759	97,00	31	1,01 (0,99-1,02)	0,48518	94,20	31
	LSC n/MNC:												
	CD26+	0,79 (0,57-1,08)	0,14154	-4,40	38	0,98 (0,61-1,58)	0,94317	-4,00	38	1,13 (0,76-1,69)	0,54385	-4,40	38
	CD25+	0,79 (0,58-1,08)	0,14425	-4,44	38	0,98 (0,62-1,55)	0,94390	-4,00	38	1,12 (0,77-1,64)	0,55050	-4,44	38
	IL1-RAP+	0,79 (0,57-1,09)	0,14405	-4,27	38	1,00 (0,64-1,57)	0,99147	-3,52	38	1,09 (0,75-1,57)	0,65271	-3,52	38
	CD56+	0,85 (0,61-1,16)	0,30312	-5,06	38	0,81 (0,51-1,31)	0,39401	-4,07	38	1,09 (0,75-1,61)	0,64514	-4,72	38
	CD93+	0,90 (0,52-1,56)	0,70640	-5,12	34	1,06 (0,39-2,84)	0,91467	-5,10	34	1,27 (0,56-2,88)	0,57466	-4,63	34
	CD69+	0,79 (0,54-1,16)	0,23042	-4,41	25	1,22 (0,79-1,88)	0,37987	-5,86	25	1,08 (0,73-1,59)	0,71798	-5,97	25
	6 marker union	0,78 (0,57-1,08)	0,13480	-4,03	38	1,01 (0,65-1,59)	0,95217	-5,95	38	1,12 (0,77-1,63)	0,53721	-4,03	38
M3	LSC %:												
	CD26+	1,32 (0,80-2,19)	0,28094	0,00	9	0,00 (0,00-Inf)	0,99951	0,00	9	0,00 (0,00-Inf)	0,99939	0,00	9
	CD25+	1,14 (0,96-1,36)	0,14664	0,00	9	0,00 (0,00-Inf)	0,99865	0,00	9	0,00 (0,00-Inf)	0,99830	0,00	9
	IL1-RAP+	0,99 (0,97-1,01)	0,24430	82,40	9	45,87 (0,00-Inf)	0,99635	78,10	9	1,02 (0,98-1,05)	0,36440	78,10	9
	CD56+	0,92 (0,80-1,07)	0,28180	3,77	9	1,15 (0,89-1,48)	0,29873	3,77	9	1,12 (0,94-1,35)	0,21212	3,77	9
	CD93+	0,94 (0,73-1,21)	0,63194	1,89	9	1,08 (0,74-1,58)	0,67592	1,89	9	1,08 (0,83-1,39)	0,58248	1,89	9
	CD69+	0,99 (0,85-1,17)	0,94008	4,00	9	0,93 (0,63-1,37)	0,70561	4,00	9	0,87 (0,59-1,28)	0,47110	4,00	9
	6 marker union	0,99 (0,97-1,01)	0,26558	87,50	9	1,18 (0,89-1,57)	0,25388	77,30	9	1,02 (0,98-1,05)	0,37392	87,50	9
	LSC n/MNC:												
	CD26+	1,17 (0,51-2,73)	0,70933	-6,46	34	2,02 (0,55-7,42)	0,29116	-5,54	34	2,34 (0,79-6,93)	0,12564	-5,76	34
	CD25+	1,24 (0,54-2,87)	0,60768	-6,46	34	2,02 (0,53-7,68)	0,29966	-5,54	34	2,17 (0,72-6,52)	0,16880	-5,76	34
	IL1-RAP+	1,35 (0,59-3,06)	0,47905	-5,11	34	1,71 (0,59-4,99)	0,32444	-5,52	34	1,39 (0,58-3,33)	0,46170	-5,52	34
	CD56+	0,94 (0,40-2,23)	0,89366	-5,47	34	3,15 (0,81-12,24)	0,09803	-5,54	34	3,15 (1,04-9,54)	0,04285	-5,76	34
	CD93+	0,85 (0,39-1,87)	0,69180	-5,47	34	3,73 (0,97-14,38)	0,05572	-5,54	34	3,50 (1,18-10,38)	0,02424	-5,76	34
	CD69+	1,34 (0,56-3,21)	0,50985	-6,46	34	1,76 (0,43-7,15)	0,43154	-5,54	34	2,06 (0,64-6,67)	0,22618	-5,76	34
	6 marker union	1,53 (0,67-3,49)	0,30961	-5,94	34	1,65 (0,54-5,10)	0,38241	-5,52	34	1,24 (0,48-3,15)	0,65756	-5,52	34
M6	LSC %:												
	CD26+	0,95 (0,80-1,12)	0,53759	4,00	13	1,24 (0,98-1,57)	0,07877	4,00	13	1,16 (0,93-1,46)	0,18321	4,00	13
	CD25+	0,94 (0,79-1,12)	0,48948	0,00	13	0,97 (0,73-1,30)	0,86213	0,00	13	1,09 (0,91-1,29)	0,34842	0,00	13
	IL1-RAP+	1,00 (0,99-1,02)	0,71381	12,90	13	1,01 (0,98-1,03)	0,53076	3,33	13	1,00 (0,98-1,02)	0,86227	3,33	13
	CD56+	0,97 (0,88-1,07)	0,59918	0,00	13	1,05 (0,94-1,18)	0,39716	3,85	13	1,03 (0,93-1,14)	0,60191	0,00	13
	CD93+	not reliable			13	not reliable			13	not reliable			13
	CD69+	not reliable			13	not reliable			13	not reliable			13
	6 marker union	not reliable			13	not reliable			13	not reliable			13
	LSC n/MNC:												
	CD26+	0,61 (0,22-1,69)	0,34150	-5,88	38	2,17 (0,52-9,06)	0,28844	-5,88	38	2,05 (0,63-6,72)	0,23504	-5,80	38
	CD25+	0,62 (0,22-1,74)	0,36746	-5,88	38	1,59 (0,38-6,71)	0,52697	-5,88	38	1,89 (0,57-6,25)	0,29878	-5,80	38
	IL1-RAP+	0,50 (0,20-1,28)	0,14931	-5,82	38	3,44 (0,84-14,15)	0,08667	-5,53	38	2,28 (0,72-7,24)	0,16118	-5,82	38
	CD56+	0,56 (0,19-1,71)	0,31044	-5,88	38	2,78 (0,64-12,20)	0,17442	-5,88	38	2,38 (0,70-8,13)	0,16576	-5,80	38
	CD93+	0,65 (0,23-1,84)	0,41749	-5,88	38	1,81 (0,43-7,55)	0,41741	-5,88	38	1,79 (0,55-5,89)	0,33480	-5,80	38
	CD69+	0,65 (0,23-1,84)	0,41749	-5,88	38	1,81 (0,43-7,55)	0,41741	-5,88	38	1,79 (0,55-5,89)	0,33480	-5,80	38
	6 marker union	0,44 (0,16-1,23)	0,11876	-5,82	38	3,20 (0,73-13,95)	0,12154	-5,20	38	2,82 (0,84-9,51)	0,09471	-5,82	38

Figure S22. Correlation of PB LSC data with patient outcomes. Univariate Cox models of LSC data for MMR, FFS, and ORS at DX, M3, M6. LSCs data are shown both as % of LSCs from CD34+CD38- fraction (LSC %) or the number of LSCs from MNC fraction (n/MNC). LSCs identification was performed based on individual markers or the 6 marker union (positivity for any marker).Red values denote differences between the evaluated models. CI – confidence interval, DX – diagnosis, FFS – failure-free survival, HR – hazard ratio, IS – international scale, LSC – leukemic stem cell, M – month, MMR – cumulative major molecular response, n – number, PB – peripheral blood, ORS – optimum response survival.

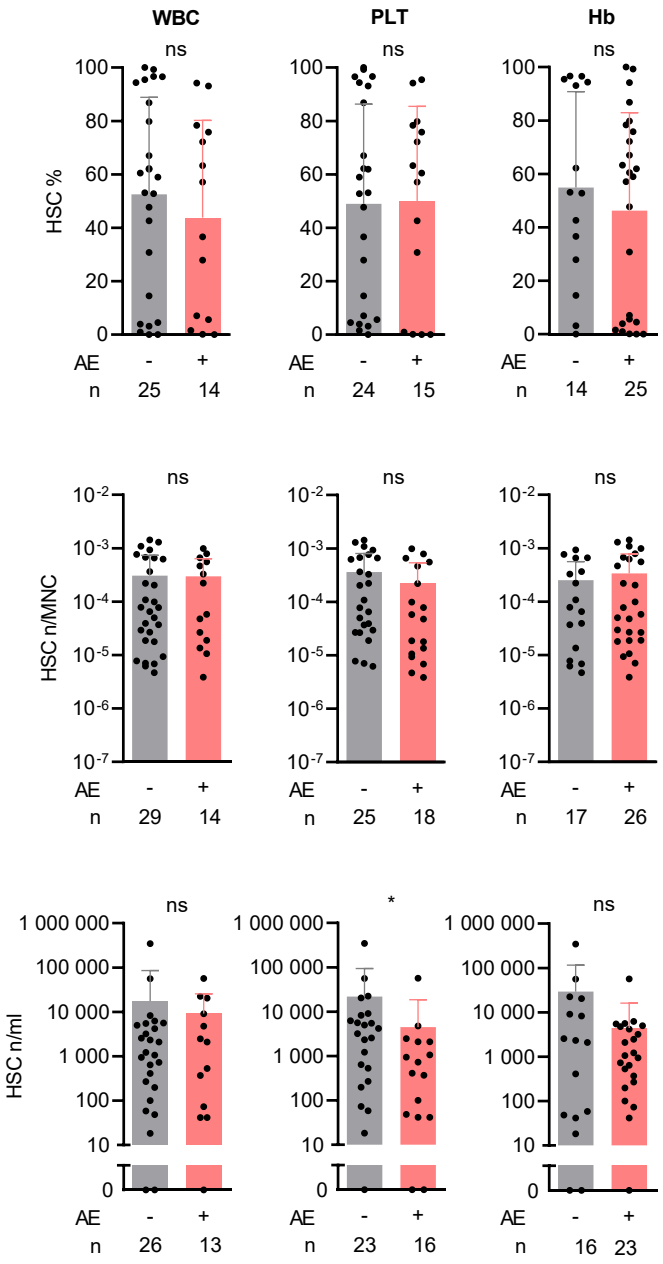

Figure S23. Correlation of hematological toxicity within the first 3 months with residual BM HSCs at diagnosis, in the main cohort of 48 CP CML patients. Patients shown as those with and without leukopenia (< 4 × 10^9 leukocytes/L), thrombocytopenia (< 150 × 10^9 platelets/L), or anemia (< 120 g/L for women, < 130 g/L for men). HSCs identified as CD34+CD38- cells negative for 6 LSC markers and quantified using three metrics: percentage of CD34+CD38- fraction (%, upper row), fraction of MNCs (n/MNC, middle row), and HSC count per 1 ml of BM (n/ml, bottom row). Unpaired, non-parametric t-test. AE – adverse event, BM – bone marrow, CP CML – chronic phase chronic myeloid leukemia, Hb – hemoglobin, HSC – normal hematopoietic stem cells, MNC – mononuclear cell, n – number/count, ns – not significant, PLT – platelets, WBC – white blood cell count. * $p < 0.05$

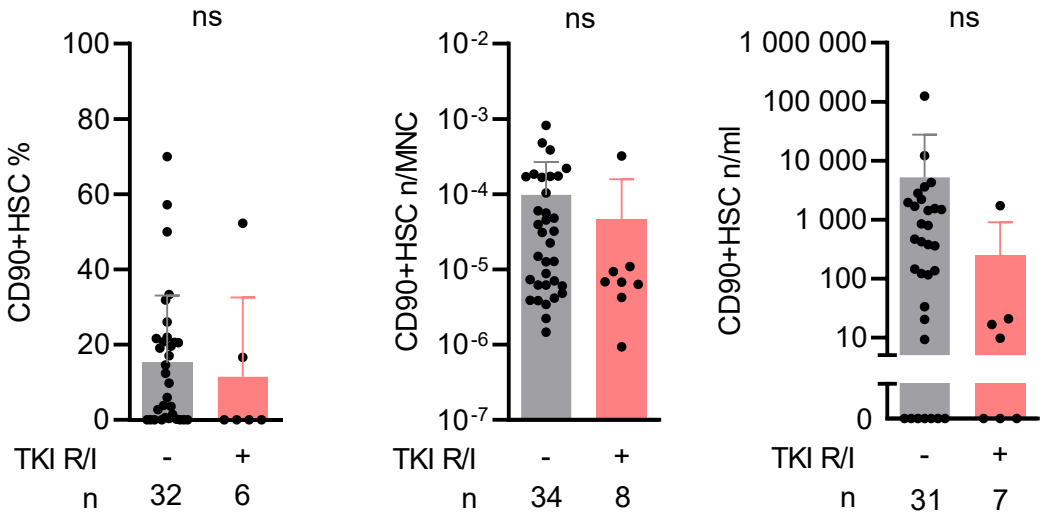

Figure S24. Correlation of CD90+ residual BM HSCs with TKI treatment modification in the main cohort of 48 CP CML patients. TKI dose reduction/interruption within the first 3 months was based on hematological toxicity. CD90+HSCs were identified as CD34+CD38-CD90+ cells lacking expression of any LSC markers. CD34+CD38-CD90+ quantification was performed using three metrics: percentage of CD34+CD38- fraction (%, left), fraction of MNCs (n/MNC, middle), and HSC count per 1 ml of BM (HSC n/ml, right). Unpaired, non-parametric t-test. BM – bone marrow, CP CML – chronic phase chronic myeloid leukemia, HSC – normal hematopoietic stem cell, MNC – mononuclear cell, n – number/count, ns – not significant, TKI R/I – tyrosine kinase inhibitor dose reduction or treatment interruption.

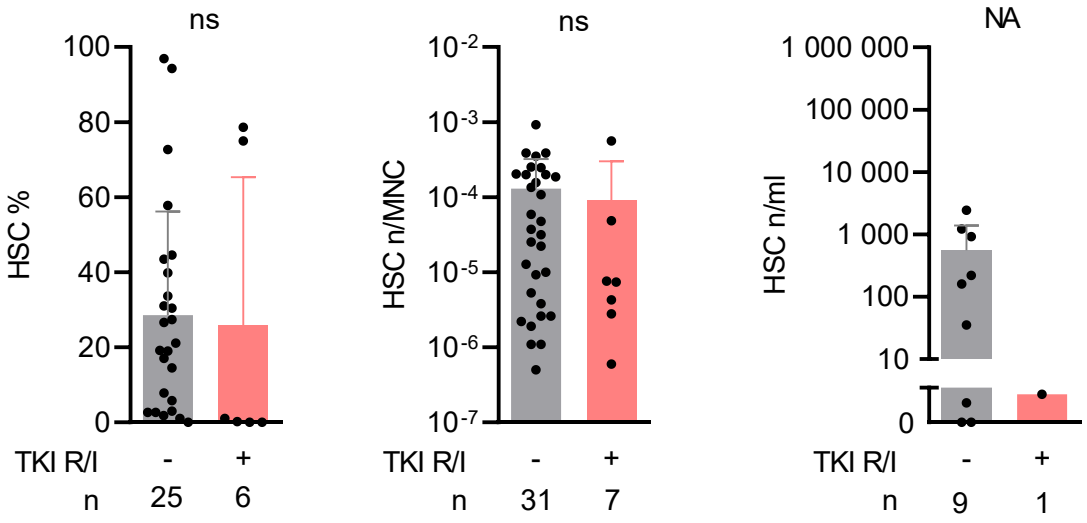

Figure S25. Correlation of residual PB HSCs with TKI treatment modification in the main cohort of 48 CP CML patients. TKI dose reduction/interruption within the first 3 months was based on hematological toxicity. HSCs were identified as CD34+CD38- cells lacking expression of any LSC marker. HSC quantification was performed using three metrics: percentage of CD34+CD38- fraction (%, left), fraction of MNCs (n/MNC, middle), and HSC count per 1 ml of PB (n/ml, right). The low sample count in HSC n/ml was caused by absence of WBC data for remaining samples. Unpaired, non-parametric t-test. CP CML – chronic phase chronic myeloid leukemia, HSC – normal hematopoietic stem cell, MNC – mononuclear cell, n – number/count, ns – not significant, PB – peripheral blood, TKI R/I – tyrosine kinase inhibitor dose reduction or treatment interruption.

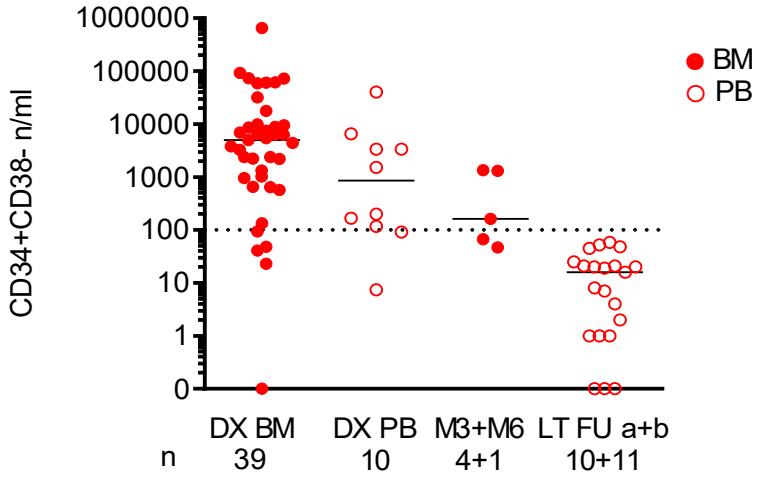

Figure S26. Quantification of CD34+CD38- cells in different materials from different time points. Only fresh samples with leukocyte counts available included. DX, M3, M6: patients from the main CML cohort. LT FU: PB samples from long-term follow-up. LT FU a: main cohort patients, year 2-5 from diagnosis, 7/10 in MMR at sampling. LT FU b: additional CP CML patients, year 2-10 from diagnosis, all in MMR or better at sampling. Line shows median values. BM – bone marrow, CP CML – chronic phase chronic myeloid leukemia DX – diagnosis, M – month, MMR – major molecular response, n – sample count, LT FU – long term follow-up, PB – peripheral blood.

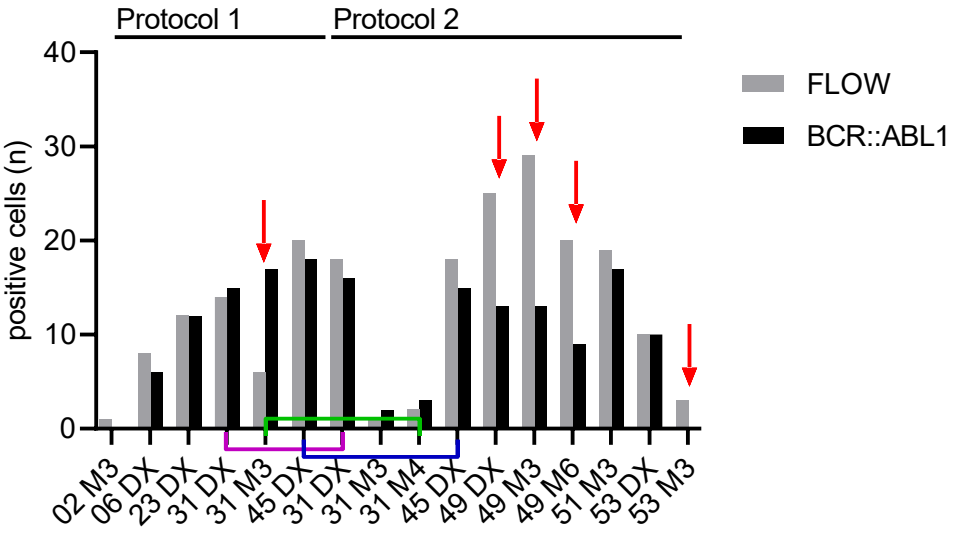

Figure S27. Comparison of two protocols for *BCR::ABL1* assessment at single-cell level (see Supplementary methods). The performance of both molecular protocols (designated as "BCR::ABL1") was compared with flow-cytometric 6 LSC marker union positivity (CD26, CD25, IL1-RAP, CD56, CD93, CD69), designated as "FLOW"). Three samples (connected using color lines around X-axis) were analyzed by both molecular protocols, however, on different days, using different aliquots. The red arrows highlight samples with the highest discrepancy between molecular and flow analysis. Protocol 2 underestimated the ratio of positive cells compared to flow cytometry in 4 samples. However, 3 of these samples originated from the same patient (different time-points). This could suggest a biological variation, such as weaker *BCR::ABL1* RNA expression or non-specific marker expression on normal stem cells, rather than a technical issue.